

Simulation of a Kicked Bose-Einstein Condensate

Diploma Thesis

Thomas Prosser
tprosser@phys.ethz.ch

To my father, who would have liked to see this completed.

Contents

1 Basics of Bose-Einstein Condensation	5
1.1 Non-Interacting Bose-Gas	5
1.1.1 Bose distribution	5
1.1.2 The Bose-Einstein Condensate in a Harmonic Trap	6
1.1.3 The Bose-Einstein Condensate in an Optical Lattice	7
1.2 Kicked Condensates	9
2 The Gross-Pitaevskii Equation	15
2.1 Interactions of Condensed Atoms	15
2.1.1 Covalent Bonds and the Van der Waals Force	15
2.1.2 Dimensional Estimate of the Scattering Length	15
2.2 Scattering theory	16
2.2.1 Basic Aspects	16
2.2.2 Partial Wave Expansion	17
2.2.3 Effective Interaction	17
2.3 The Gross-Pitaevskii Equation	18
2.4 Ground State for Trapped Bosons	19
2.4.1 Variational Calculation for the Ground State	19
2.4.2 Generalisation of the Gross-Pitaevskii Equation	22
3 Numerical Methods	23
3.1 General Considerations	23
3.2 The Gross-Pitaevskii Equation	24
3.2.1 The Framework	24
3.2.2 Finding the Groundstate Using the Split-Step Operator Method	25
3.3 The Code	27
3.3.1 C++-Code for the Split-Step Operator Method	27
3.3.2 Perl code	28
4 Results	29
4.1 The System under consideration	29
4.2 “Phase Space” Plots of the BEC	29

4.3	Momentum Distributions at Various Times	32
4.4	Widths of Momentum Distributions	34
4.4.1	The Exponentially Weighted Moving Average.	34
4.4.2	Widths	34
4.5	Conclusion	44

Introduction

In 1925, Einstein predicted that at low temperatures, particles in a gas could reside in precisely the same quantum state. This state however, now referred to as a Bose-Einstein Condensate (BEC), was produced only very recently, in 1995 [1] with about 2000 ^{87}Rb -Atoms in a quadrupole trap. As the name suggests, this state can only be observed with bosons (after S. N. Bose, who put forward the fundamental distribution function of particles having integer spin), since for fermions, the Pauli exclusion principle prohibits two spin- $\frac{1}{2}$ particles in exactly the same quantum state. This work considers a BEC in one dimension at absolute zero, residing in both an optical lattice and a harmonic trap. This theoretical system is subsequently kicked, i.e. energy is conveyed to the system and it is numerically propagated in time. The effect seen will be a phase decoherence, visible in the broadening of the momentum distribution as a consequence of the nonlinearity of the Gross-Pitaevskii equation governing the behaviour of the condensate at low temperatures; Unlike the normal Schrödinger equation which is linear, the Gross-Pitaevskii equation exhibits a nonlinear term to include interactions between the atoms in the condensate. This nonlinearity is responsible for the instability of the system in the above sense when kicked strong enough.

Chapter 1

Basics of Bose-Einstein Condensation

1.1 Non-Interacting Bose-Gas

The theory of the non-interacting Bose Gas is developed in full in most textbooks on statistical mechanics, so the reader is referred to them for more information about how to calculate the proper statistics. We only want to recall the results briefly.

1.1.1 Bose distribution

By considering a grand canonical ensemble for bosons [10] one arrives at the familiar energy distribution function:

$$f(\varepsilon_n) = \frac{1}{e^{\frac{\varepsilon_n - \mu}{k_B T}} - 1} \quad (1.1)$$

Where ε_n denotes the Energies of the single-particle eigenstates of the system, and μ is the chemical potential. For high temperatures, the chemical potential is considerably smaller than the minimal energy of the system, as there are very few particles in the same state. As temperature falls however, the chemical potential gets comparable to this minimal energy, yet cannot exceed it for the reason that equation (1.1) would be negative, which is clearly non-physical. As a consequence, the occupation number of any excited single-particle state cannot exceed the value $\frac{1}{e^{\varepsilon_n - \varepsilon_{min}/k_B T} - 1}$. This accounts for the fact that if we consider N particles of which less than N are in an excited state, the remaining particles have to be accommodated in the lowest state, the system is then said to exhibit Bose-Einstein condensation.

6 CHAPTER 1. BASICS OF BOSE-EINSTEIN CONDENSATION

1.1.2 The Bose-Einstein Condensate in a Harmonic Trap

Bose-Einstein Condensates are usually produced inside a magnetic or optical trap. The first BEC was cooled using laser-cooling for the atoms to be slow enough to be held in a magnetic (quadrupole) trap. For details and various implementations of several traps, the reader is referred to [17], as well as to the original article by Anderson et. al. [1]. The traps usually introduce a harmonic potential to the overall Hamiltonian of the system. In our case, we consider a potential of the form:

$$V(x) = \frac{x^2}{2} \quad (1.2)$$

Which is the potential one would find for a normal harmonic oscillator. Indeed, if we consider single-particle states of bosons and choose units so that $\hbar = 1$ and the mass $m = 1$, the Hamiltonian for a single particle (and hence for an arbitrary number of particles all in the same single particle ground state) reads:

$$\hat{H} = -\frac{1}{2} \frac{d^2}{dx^2} + V(x) \quad (1.3)$$

The solution to the Schrödinger equation for this System is familiar from standard Quantum Mechanics textbooks ¹, and it suffices to state that the Groundstate of this system is described in position space by the wave-function:

$$\frac{1}{\pi^{1/4}} e^{-\frac{x^2}{2}} \quad (1.4)$$

which is already normalized to unity. The fact that this system is soluble analytically provides an excellent means of checking the results of the numerical simulations for correctness of the code. However, this treatment does not account for the fact that in real condensates, there are actually interactions between the particles and that these interactions are very peculiar to the nature of the atoms in the condensate. As this system has stationary states, they do not change and the condensate would therefore stay in exactly this same state. Moreover, as the minimal energy is given and all the particles would come to the minimal energy state, the system would be in its ground state, having no fluctuations at all. In this work, we consider a one-dimensional condensate. Such a system was only recently (2003) realized [16], which gives the system at hand a practical relevance. It is different from the three-dimensional condensate in that it cannot exist at finite temperatures. This fact is a direct consequence of the Mermin-Wagner-Hohenberg Theorem, which basically states that there cannot be any spontaneous symmetry breaking at finite temperature for one- or two-dimensional systems. A proof for the theorem can be found in the original work [15], applied to magnetic systems. Two years later, Hohenberg [9] pointed

¹A very thorough introduction is given in [20]

out that in the case of a superliquid, the theorem also applies since in a superliquid (and in a Bose-Einstein condensate, for that matter), all particles carry exactly the same momentum, which means that the symmetry of such a system is effectively broken. This however cannot occur for a one-dimensional system at finite temperature. For the calculations, I refer the reader to the above cited articles.

1.1.3 The Bose-Einstein Condensate in an Optical Lattice

Instead of only confining the Bose-Einstein condensate in a trap of the form (1.5), it is also possible to use a potential of the form

$$\hat{V}_{\text{lattice}} = s \frac{q_B^2}{2} \sin^2(qx) \quad (1.5)$$

where s is some parameter to control the intensity of the lattice. As the name suggests, the lattice is formed by means of lasers, the electric field will be of the form $E_0 \sin(qx) \sin(\omega t)$, where q is just the wave vector of the incident laser light, $q = \frac{2\pi}{\lambda}$. As we will see, Bose-Einstein Condensates follow the Gross-Pitaevskii equation (2.16). A solution for the Ground-state for this equation in the one-dimensional case can be given in terms of its Fourier series:

$$\psi_0 = \sum_{l=0,\pm 1,\dots} \psi_l e^{\frac{il2\pi x}{d}} \quad (1.6)$$

d being the lattice constant, $d = \frac{\lambda}{2}$, and $\psi_l = \frac{1}{d} \int_{-\frac{d}{2}}^{\frac{d}{2}} \psi_0 e^{-\frac{il2\pi z}{d}} dz$, as usual. The behaviour of the wave function is best shown in momentum space. Thus, we form the Fourier transform of the above function, again using units such that $\hbar = 1$:

$$\begin{aligned} \psi_0(p) &= \int_{-\infty}^{\infty} \sum_{l=0,\pm 1,\dots} \psi_l e^{\frac{il2\pi lx}{d}} e^{-ipx} dx \\ &= \sum_{l=0,\pm 1,\dots} \psi_l \int_{-\infty}^{\infty} e^{-ix(p - \frac{il2\pi l}{d})} dx \\ &= 2\pi \sum_{l=0,\pm 1,\dots} \psi_l \delta(p - \frac{2\pi l}{d}) \end{aligned}$$

Thus, it is seen that the momentum distribution is given by a sum of delta peaks. However, we want to consider a condensate that is kicked, so we have to incorporate some means of kicking, which is experimentally done by tilting the trap out of the axis for a short time. Therefore, apart from the lattice, we also have to add a trap. This however is just the superposition of two potential terms. The lattice in the potential was added by simply adding the term $\frac{q_B^2}{2} \sin^2(q_B x)$ [14], where q_B is the wavevector at the boundary of the first Brillouin zone, $q_B = \frac{\pi}{a}$ and a is

8 CHAPTER 1. BASICS OF BOSE-EINSTEIN CONDENSATION

the lattice constant. The Groundstate of such a potential is shown in the figures below. The form of the lattice is not arbitrary. The factor $\frac{q_B^2}{2}$ arises, because of the recoil energy an atom acquires when absorbing a photon with momentum q . As the field produced by a laser which is normally used to produce a lattice is $E_0 \sin(qx) \sin(\omega t)$, the time-averaged field is then proportional to $\sin^2(qx)$ [18]. It has to be noted, that the dynamics are non-trivial, because of the nonlinearity that arises from the interatomic interactions. It is most fitting to use numerical techniques. The following pictures will illustrate the nature of the Ground state further. Let now the potential be of the form above, and let the atoms be trapped with the normal harmonic potential. The overall external potential is then periodic. Let again $\psi(x)$ be the wavefunction of a one dimensional Bose-Einstein condensate still obeying the equation (2.16). As is explained above, Figures 1.1 and 1.2 show the first two sattelite peaks, that are obtained in precisely this way.

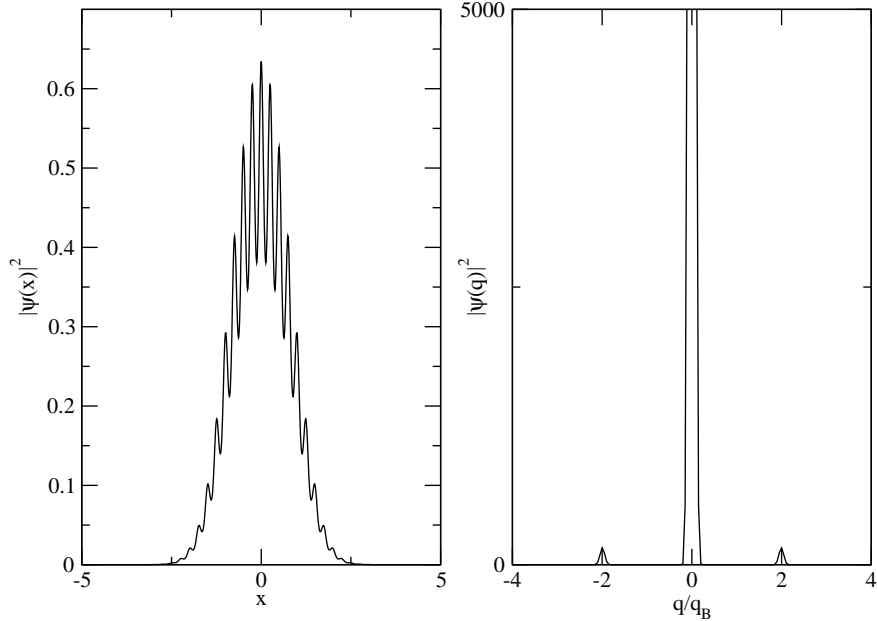


Figure 1.1: Ground state distribution of a Bose-Einstein condensate in a periodic potential and its corresponding momentum distribution with $g = 1$

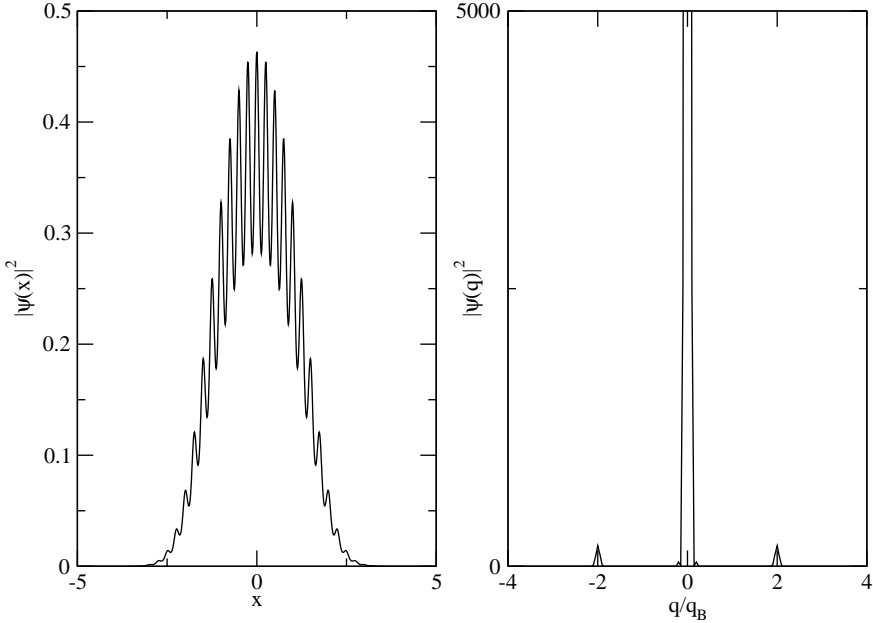


Figure 1.2: Same as figure 1.1 with $g = 5$

1.2 Kicked Condensates

A kick in theory is introduced by a delta peak [19], having a given kick strength K . In our split-step operator framework, this is equal to multiplying the wavefunction with a phase factor, thereby leaving its norm untouched. My starting point was the delta-kicked rotor, already analyzed in [19] and recently treated quantum mechanically in [23], where it was shown using a split-step operator technique, that for larger couplings between the atoms, the system undergoes a transition to chaos when kicked periodically. Such a system is very close to the above mentioned delta-kicked rotor in that as the interactions in the mean-field approximation add a nonlinear term to the Schrödinger equation. This will render the system open to chaotic, or unstable behaviour. Chaos is usually not possible in Quantum Mechanics, because of the linearity of the Schrödinger equation, and it is generally disputed whether or not one can speak of chaos in Quantum Mechanics, since the classical definition, e.g. via Lyapounov-exponents [2], requires some notion of a trajectory, which is naturally absent in Quantum Mechanics. However, a nonlinear Schrödinger equation exhibits exponential sensitivity to

initial conditions. As [23] shows, a one-dimensional Bose-Einstein Condensate which is confined to a ring and is then periodically kicked, can exhibit quantum anti-resonance (periodic recurrence between different states), which is destroyed for large enough coupling constants that render the nonlinearity appreciable. Figure 1.3 shows quantum anti-resonance and its disappearance when the coupling becomes strong enough

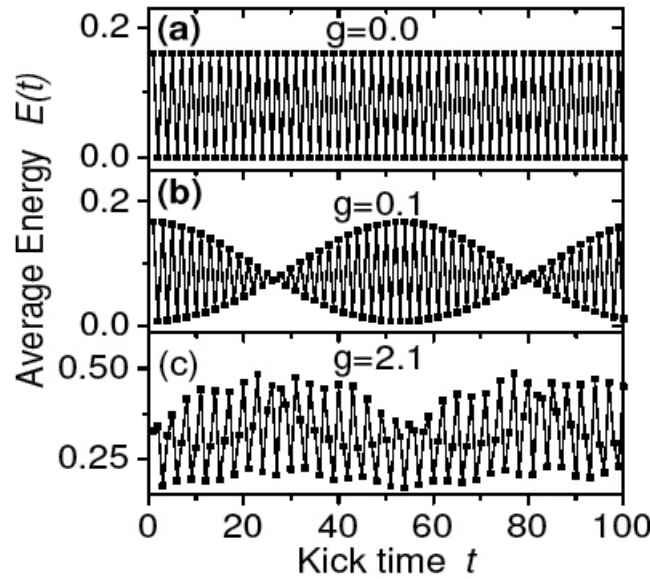


Figure 1.3: Average energy of a BEC confined to a ring. The nonlinearity destroys quantum anti-resonance. Taken from [23]

This work examines the effects of a condensate in a trap with an optical lattice superimposed. The condensate is kicked once and subsequently left to its own and it is assumed that the Gross-Pitaevskii equation still holds. The propagation is done using a split-step operator technique both for finding the ground state and propagating the system in time. The result will be phase decoherence in momentum-space, owing to the nonlinear term in the Gross-Pitaevskii equation, if only the kick that is exerted is strong enough for a given coupling constant. For our purposes, the kick was given by $K \sin(x)\delta(t_k)$, which could be realized in a physical system by tilting the trap in which the condensate is contained out of place for a short time. When converting this into an exponential operator, it is seen that for the split-step technique applied to solve this system, we have to multiply our wave function by the factor $e^{-iK \sin(x)}$, since the kick is taken to be instantaneous at an arbitrary chosen time t_k . As can be analytically shown in the case of the Gross-Pitaevskii equation with no interaction between the atoms,

this shifts the momentum-distribution to the right: Our analytical system reads:

$$\left(-\frac{1}{2} \frac{d^2\psi}{dx^2} + \frac{x^2}{2} \right) \psi = E\psi \quad (1.7)$$

This has the very familiar solution $\psi = \frac{1}{\pi^{\frac{1}{4}}} e^{-\frac{x^2}{2}}$. The mean momentum after applying a kick is obtained by observing that:

$$\begin{aligned} \langle p \rangle &= \frac{1}{i\pi^{\frac{1}{2}}} \int_{-\infty}^{\infty} (x + iK \cos x) e^{-x^2} dx \\ &= \frac{1}{\pi^{\frac{1}{2}}} \int_{-\infty}^{\infty} K \cos(x) e^{-x^2} dx \\ &= \frac{K}{\sqrt{\pi} e^{\frac{1}{4}}} \operatorname{Re} \left(\int_{-\infty}^{\infty} e^{-(x-\frac{i}{2})^2} dx \right) \\ &= \frac{K}{e^{\frac{1}{4}}} = 0.77880 \cdot K \end{aligned} \quad (1.8)$$

This result was mainly mentioned because it serves as a test to the software used; If one kicks a harmonic oscillator in the right way, then the shift in momentum should be exactly the above constant. Furthermore, it serves as a rough estimate on the orders of magnitude of the momentum shift a kick introduces. From this simple calculation, we can then deduce, that the fundamental effect a kick has on a Bose Einstein condensate is to shift its momentum slightly to the right of momentum space, by an amount that is proportional to the Kick strength. One can also see that a symmetric kick, e.g. $e^{-iK \cos x}$ would have had no effect on the mean momentum at all.

Furthermore, we want for the sake of completeness give an analytic estimate for $\langle p^2 \rangle$, since it will be important when considering the mean width of the distribution, calculated by $\langle p^2 \rangle - \langle p \rangle^2$. We thus proceed along the same lines:

$$\begin{aligned} \langle p^2 \rangle &= -\frac{1}{\pi^{\frac{1}{2}}} \int_{-\infty}^{\infty} e^{-x^2} [(-x + iK \cos(x))^2 + (-1 - iK \sin(x))] \\ &= \frac{K^2 + e(K^2 - 1)}{2e} + 1 \end{aligned} \quad (1.9)$$

After a somewhat lengthy calculation that proceeds as the one for (1.8), dropping the sine term and integrating the rest as was shown before. The variance can now be given as:

$$\langle p^2 \rangle - \langle p \rangle^2 = \frac{e + (1 - 2\sqrt{e} + e)K^2}{2e} = \sigma^2 \quad (1.10)$$

For a normal BEC in a trap having no interaction, this yields a variance of 0.577409 at kick strength $K = 1$, which was confirmed by a numerical computation of width and mean of the distribution in figure 1.4. A point on units has to

12 CHAPTER 1. BASICS OF BOSE-EINSTEIN CONDENSATION

be made. As I am using a fast Fourier Transform to calculate momentum distributions, the momenta vary from $-\frac{\pi N}{L}$ to $\frac{\pi N}{L}$, where N is the number of points used and L is the overall system size considered. I chose $N = 1024$ and $L = 10$ to be fitting values for our purposes. As mentioned, the spectrum of momenta is discrete and the unit of momentum would be $\frac{2\pi N}{LN} = \frac{\pi}{5}$. In order to get rid of factors of π , One can choose the momentum at the boundary of the Brillouin-zone, $q_B = \frac{40\pi}{L}$ as a unit of measurement. This yields a much more comfortable unit for momenta and where not stated otherwise, these units are used.

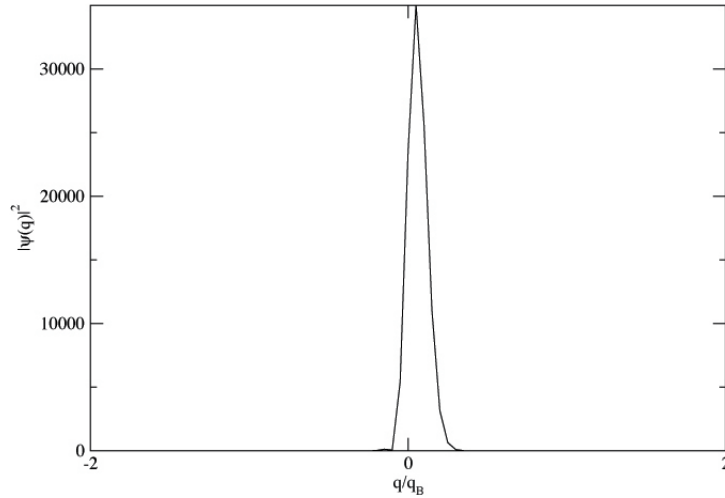


Figure 1.4: A one dimensional Bose-Einstein Condensate kicked with a strength $K = 1$. Note the slight shift to the right. With the `analyze` Perl script, the mean momentum was found to be $\langle p \rangle = 0.778801$, which in the above units is at roughly 0.06 and $\langle p^2 \rangle - \langle p \rangle^2 = 0.577409$, which would be about 0.05. Although no Brillouin-zone is present, I chose to normalize with the Brillouin vector, in order to get rid of factors of π .

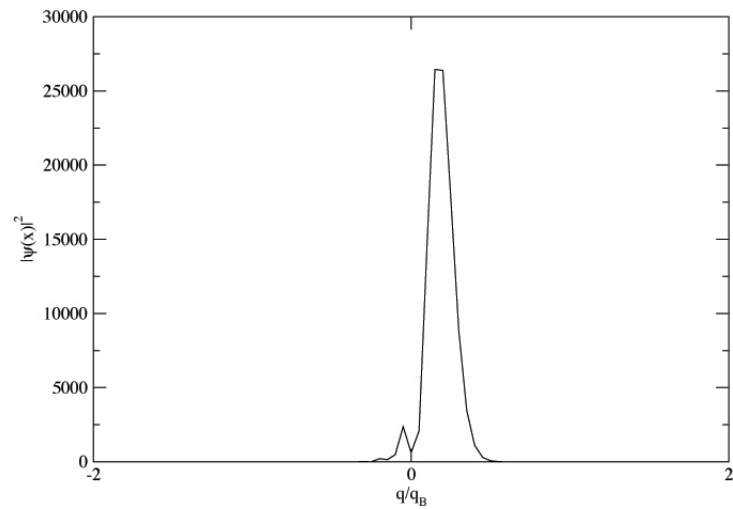


Figure 1.5: A one-dimensional BEC kicked with $K = 5$, $\langle p \rangle \approx 0.19$ and $\langle p^2 \rangle - \langle p \rangle^2 \approx 0.09$

14 CHAPTER 1. BASICS OF BOSE-EINSTEIN CONDENSATION

Chapter 2

The Gross-Pitaevskii Equation

2.1 Interactions of Condensed Atoms

In order to derive the Gross-Pitaevskii equation, we will briefly consider the nature of interactions within the condensate. This will basically lead us to recalling scattering theory from basic quantum mechanics [20]. Since most of the condensates formed to this day were realized with alkali atoms, a treatment in terms of these is widely accepted. The scattering length a is of the order of 100 Bohr radii, which means that clouds formed with alkali atoms are dilute in the sense that at any time there is mainly two-particle scattering.

2.1.1 Covalent Bonds and the Van der Waals Force

When considering polarized atoms such as alkali atoms, one has to bear in mind that since the outer electrons of two different atoms can have opposite spin, they can occupy the same orbital and give therefore an attractive component. This of course is the origin of the covalent bond between atoms. At large distances, there is the Van der Waals force between atoms, which has its origin in the electric dipole-dipole interaction of the electrons which is however much weaker than that of covalent bonding. Still, as there are more triplet than singlet states for two electrons, and only singlet states can exhibit a covalent bond for two electrons, the Van der Waals force becomes strong in this sense, as in a triplet state, the Pauli exclusion principle prohibits two electrons of the same spin state to be in the same orbital.

2.1.2 Dimensional Estimate of the Scattering Length

All two-body interactions are characterized by the scattering lengths of atoms which one can estimate by a simple dimensional argument, [17]. We have the kinetic energy $\approx \frac{\hbar^2}{mr_0^2}$, where r_0 is calculated from the Schrödinger equation to

be the distance of minimal energy. The electric field of a dipole is roughly $\approx \frac{p_1}{r_0^3}$ where p_1 is the dipole moment of the dipole. The induced moment of this dipole, p_2 , on another dipole is in turn proportional to the field strength, its energy being thereby proportional to the square of the electric field of the first dipole, as $p_2 \approx |E|$ and $U \approx -p_2|E| \Rightarrow U \approx -\frac{\alpha}{r_0^6}$, whereby we have effectively estimated the Van der Waals energy, and α is some constant introduced on dimensional grounds. Equating the two energies, we get a value of $(\frac{\alpha m}{\hbar})^{\frac{1}{4}}$ for r_0 . α must be of the form of a typical atomic energy, given by the normal Coulomb form $\frac{e^2}{a_0}$, where a_0 is the Bohr radius. To get an energy out of our original form of the Van der Waals potential, we have to multiply this by the sixth power of the atomic length scale a_0 , and thus $\alpha = C_6 e_0^2 a_0^5$:

$$r_0 \approx \left(C_6 \frac{m}{m_e} \right)^{\frac{1}{4}} a_0 \quad (2.1)$$

Which gives us a general magnitude of the scattering length. For alkali atoms, C_6 is given e. g. in [6]. The sign of the interaction is however determined by the short range part, where covalent bonds can be attractive. For alkali atoms, the Van der Waals coefficients are of the order of 10^3 , so a typical scattering length is of order $10^2 a_0$.

2.2 Scattering theory

2.2.1 Basic Aspects

In order to introduce the scattering length of a system, we review quickly some calculations from standard textbooks. For a more thorough treatment, the reader is referred to [20]. Usually, one considers the eigenstates of the Schrödinger equation with energies $E_k = \frac{\hbar^2 k^2}{2m} \geq 0$ and a certain Potential $V_{scatt}(x)$

$$\left[-\frac{\hbar^2}{2m} \frac{d^2}{dx^2} + V_{scatt}(x) - E_k \right] \psi_k = 0 \quad (2.2)$$

The exact solution of this equation can be found by using Greens' functions, but one usually considers only distances far away from where the scattering takes place. This might be familiar from the situation of Fraunhofer diffraction. One can then write the wave function in the form:

$$\psi_k(x) = e^{ikx} + \frac{e^{ikr}}{r} f_k(\vartheta, \varphi) \quad (2.3)$$

$$f_k(\vartheta, \varphi) = -\frac{m}{2\pi\hbar^2} \int d^3x' e^{-i\mathbf{k}'\mathbf{x}'} V(\mathbf{x}') \psi_k(\mathbf{x}') \quad (2.4)$$

Where now the scattering amplitude f does only depend on direction, rather than distance. Effectively, the differential cross-section of scattering is given by:

$$\frac{d\sigma}{d\Omega} = |f(\vartheta, \varphi)|^2 \quad (2.5)$$

Since we are concerned only with low energies, one can consider only s-wave scattering, in which case $f(\vartheta)$ reduces to a constant, since the process is now purely symmetric about the scattering axis. This constant is usually denoted by $-a$. The limit of low energies means that $k \rightarrow 0$, which in turn reduces the two exponentials in (2.3) to unity, so that a wavefunction in this limit takes the simple form:

$$\psi = 1 - \frac{a}{r} \quad (2.6)$$

2.2.2 Partial Wave Expansion

We briefly recall a fundamental relation of mathematical physics:

$$e^{i\mathbf{k}\mathbf{x}} = 4\pi \sum_{l=0}^{\infty} \sum_{m=-l}^l i^l j_l(kr) Y_{lm}(\Omega_k)^* Y_{lm}(\Omega_x) \quad (2.7)$$

where j_l is the spherical Bessel function, and $\Omega_{k,x}$ are solid angles in momentum and coordinate space, respectively. We can assume that the particle is incident on the z -axis and drop the φ -dependence of f . We can then expand f in terms of Legendre-polynomials:

$$f_k(\vartheta) = \sum_{l=0}^{\infty} (2l+1) f_l P_l(\cos \vartheta) \quad (2.8)$$

with the partial wave amplitudes f_l . For a spherically symmetric solution of (2.2), one can always expand: $\psi_k = \sum_{l=0}^{\infty} i^l (2l+1) R_l(r) P_l(\cos \vartheta)$, because now, the wavefunction does no longer depend on the azimuthal angle. R_l is given in terms of spherical Hankel and Bessel functions, yet we wish to shortcut the somewhat lengthy calculation found in most textbooks on quantum mechanics and briefly state that for weak potentials we have $R_l \approx j_l(kr)$. Furthermore, the same calculation finds $f_l = \frac{e^{i\delta_l} \sin \delta_l}{k}$ where δ_l are the relative phase shifts a given partial wave experiences during scattering.

2.2.3 Effective Interaction

Plugging (2.7) and (2.8) into (2.4), one arrives after a short calculation [20] at:

$$f_k(\vartheta) = \sum_{l=0}^{\infty} (2l+1) P_l(\cos \vartheta) f_l \quad (2.9)$$

$$f_l = -\frac{2m}{\hbar^2} \int dr r^2 v(r) j_l(kr) R_l(r) \quad (2.10)$$

The fact that the scattering lengths of alkali atoms are rather large compared to atomic scales enables us to go to large distances, where the potential is weak enough for R_l to be approximated by $j_l(kr)$. This means that the scattering process happens with large impact parameters which in turn means that l is large. This is the condition for the Born approximation to apply. The Born approximation basically states that:

$$f_k(\vartheta) = -\frac{m}{2\pi\hbar^2}v(\mathbf{k} - \mathbf{k}') \quad (2.11)$$

The scattering amplitude is given by the Fourier transform of our potential. When atoms are close together, interactions become very strong. In dilute gases however, this case is very unlikely and the strength of the interactions is small for typical separations. Accordingly, the wave-function is very smooth and varies slowly over space. Should however two atoms come close together, a rapid varying of the wavefunction is to be expected, and one would have to include the short range variations in the calculations. This is however rather impractical, so one introduces the concept of an effective interaction, very similar to the case of an ‘effective’ magnetisation when considering mean-field theory and averaging over all moments surrounding the considered site, rather than forming an average over every possible configuration. The key point here is that short range variations are expected to average out when the system is considered at a larger scale, which means that one keeps the large wavelengths and therefore low energies. In the limit $k \rightarrow 0$, $v(k)$ becomes a constant and we have constant f_k . By this limiting procedure, one can identify a in (2.6):

$$a = \frac{m}{4\pi\hbar^2}v(0) \quad (2.12)$$

Thus, the interaction to lowest order is essentially given by the scattering length of the atoms. This result will be important in what is going to follow.

2.3 The Gross-Pitaevskii Equation

The effective interaction between two bosons for low energies is as was shown above, constant in its momentum representation, $U_0 = \frac{4\pi\hbar^2 a}{m}$. In coordinate space, this is a contact, or on-site interaction, $U = U_0\delta(\mathbf{r} - \mathbf{r}')$. As we are dealing with a many-body problem for bosons, we adopt a mean-field approach, which accounts for the interactions of one particle with its surrounding particles by a local density, $\varrho(\mathbf{r}) = |\psi|^2$. Let $\phi(\mathbf{r})$ be a single particle wavefunction. We can then form the Hartree wavefunction by calculating:

$$\Psi = \prod_{i=1}^N \phi(\mathbf{r}_i) \quad (2.13)$$

Here, N is the particle number and \mathbf{r}_i are the coordinates of the i -th particle, respectively. Normalisation to unity is understood. As always when using a Hartree-like wavefunction, one has to bear in mind that it does not take into account the correlations of atoms, which is a basic feature of course of Bose-Einstein condensation. We therefore account for correlations with the potential U_0 . If we now let V be a potential of e.g. a trap, then the Hamiltonian of our many-particle system reads:

$$\hat{H} = \sum_{i=1}^N \left[\frac{\hat{\mathbf{p}}_i^2}{2m} + V(\mathbf{r}_i) \right] + U_0 \sum_{i < j} \delta(\mathbf{r}_i - \mathbf{r}_j) \quad (2.14)$$

When plugging (2.13) into (2.14), and then integrating the resulting stationary Schrödinger equation over all space, we get the energy

$$E = N \int d\mathbf{r} \left[\frac{\hbar^2}{2m} |\nabla \phi(\mathbf{r})|^2 + V(\mathbf{r}) |\phi(\mathbf{r})|^2 + \frac{N-1}{2} U_0 |\phi(\mathbf{r})|^4 \right] \quad (2.15)$$

Since we have the additional constraint on the particle number, $\int_{-\infty}^{\infty} |\phi|^2 dx = N$, we can take ϕ and ϕ^* to be arbitrary. If we now form the variation of $E - \mu N$ with respect to ϕ^* , we arrive at the condition for the functional to be at minimal energy:

$$-\frac{\hbar^2}{2m} \nabla^2 \phi(\mathbf{r}) + V(\mathbf{r}) \phi(\mathbf{r}) + U_0 |\phi(\mathbf{r})|^2 \phi(\mathbf{r}) = \mu \phi(\mathbf{r}) \quad (2.16)$$

Which is generally known as the time-independent Gross-Pitaevskii equation. Note that unlike the Schrödinger equation, (2.16) has the chemical potential as an eigenvalue. For Bose-Einstein condensates in which there is no interaction whatsoever between bosons, this is equal to the energy per particle, for interacting particles however, it is not.

2.4 Ground State for Trapped Bosons

[17] gives solutions to (2.16) in terms of either a Gaussian function for low interactions or a Thomas-Fermi approximation for large ones. This agrees with the fact that when there is no interaction, The ground-state of trapped bosons is given by a Gaussian function, whereas with large interaction, the condensate tends to ‘spread’ out within the trap, which can be imagined as bosons scattering each other and thereby continually spreading out. For our purposes, it is sufficient to consider a variational calculation using a gaussian trial function in one dimension.

2.4.1 Variational Calculation for the Ground State

We use a Gaussian trial function of the form $\psi(x) = \frac{1}{\sqrt{a\pi^{\frac{1}{4}}}} e^{-\frac{x^2}{2a^2}}$, as one would expect for the normal harmonic oscillator. As was previously mentioned, the

interactions basically affect the dimensions of the cloud, which can clearly be seen in figure 2.2. Plugging the above formula into (2.15), we obtain for the energy per particle:

$$E = \frac{N}{4a^2} + \frac{Na^2}{4} + \frac{N^2U_0}{2\sqrt{2\pi}a} \quad (2.17)$$

Minimizing this with respect to a shows a strong dependence on U_0 and if we leave the interaction away, we can recover the usual value for a^2 , 1 in our case. With this, the wavefunction will be a good approximation as long as the interaction energy is lower than the groundstate energy, which is given here by $\frac{N}{2}$. This can be seen by again setting a equal to one and observing that

$$\begin{aligned} E &= N \left(\frac{1}{2} + \frac{NU_0}{2\sqrt{2\pi}} \right) \\ &= \frac{N}{2} + \frac{N^2U_0}{2} \int_{-\infty}^{\infty} |\psi(x)|^4 dx \\ &= E_0 + \langle 0|v|0 \rangle \end{aligned}$$

where we have taken v to be the nonlinear part of the Gross-Pitaevskii equation. With this short calculation we have shown that we in fact made a perturbational expansion to first order for the nonlinear interaction term. This is however only valid when v is small compared to the groundstate energy E_0 . One can clearly see, that the effect of the interaction between atoms is to “smear” out the Wavefunction. Figure 2.1, shows the dependence of a on the coupling. Figure 2.2 shows the numerical calculation of the ground state of the system in one dimension to illustrate the effect of interaction between atoms. As is seen even from this simple calculation, the interaction drives atoms apart, which is what one would expect for a repulsive interaction. Consequently, one also expects a more narrow momentum distribution when changing to momentum space.

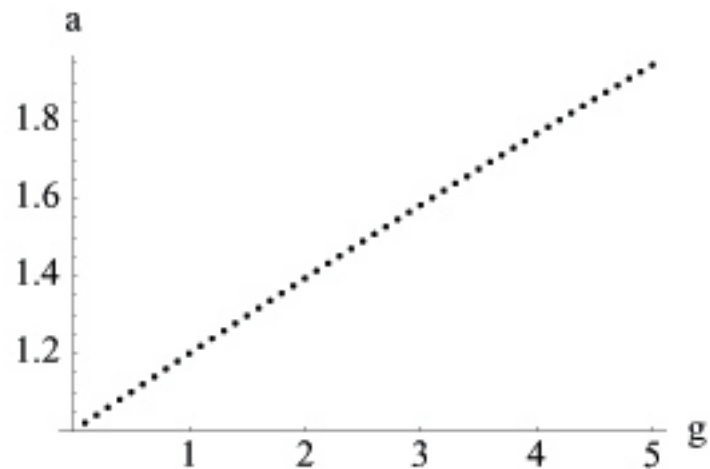


Figure 2.1: The effect of a finite inter-particle interaction is to move the atoms apart. For the particular normalization to unity, the dependence is approximately linear.

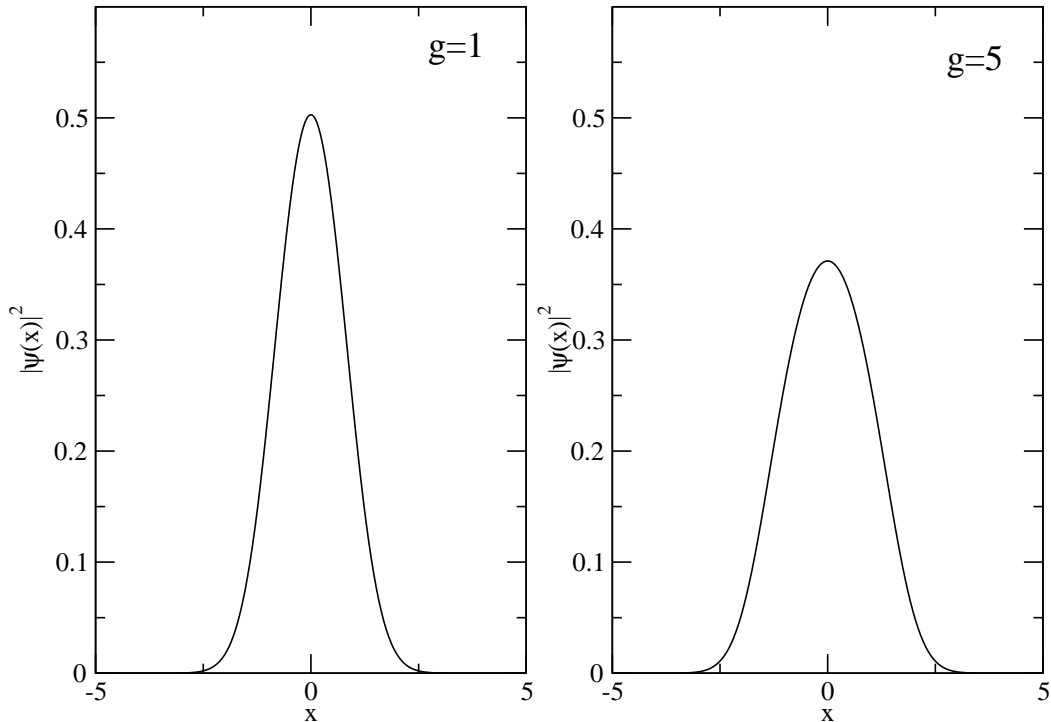


Figure 2.2: Ground state distributions for two different interaction strengths. No optical lattice has yet been applied

2.4.2 Generalisation of the Gross-Pitaevskii Equation

Equation (2.16) has the form of a Schrödinger equation with a nonlinear distribution that takes into account the interactions between particles. However, as we wish to study a kicked condensate that evolves in time, we have to move to a time-dependent equation of motion for such a condensate. The time-dependent Gross-Pitaevskii equation is given by:

$$-\frac{\hbar^2}{2m} \nabla^2 \psi(\mathbf{r}, t) + V(\mathbf{r})\psi(\mathbf{r}, t) + U_0|\psi(\mathbf{r}, t)|^2\psi(\mathbf{r}, t) = i\hbar \frac{\partial \psi(\mathbf{r}, t)}{\partial t} \quad (2.18)$$

Chapter 3

Numerical Methods

3.1 General Considerations

We want to propagate the Gross-Pitaevskii equation in time. Therefore we need an efficient algorithm to do so. The method of choice was the so-called split-step operator method, which is based on the fact that a *time-independent* Hamiltonian has an exact solution given by the time-evolution operator. The idea is to take apart the Hamiltonian in two parts.

$$i \frac{\partial \psi(x, t)}{\partial t} = \left(-\frac{1}{2} \frac{\partial^2}{\partial x^2} + V(x) \right) \psi = (\hat{A} + \hat{B}) \psi(x, t) \quad (3.1)$$

where $\hat{A} = -\frac{1}{2} \frac{\partial^2}{\partial x^2}$ and $\hat{B} = V(x)$. With that, we can write the formal solution of (3.1) as

$$\psi(x, t + \Delta t) = e^{-i\Delta t(\hat{A} + \hat{B})} \psi(x, t) \quad (3.2)$$

It has to be noted however, that this solution is no longer exact as V becomes itself time-dependent [3], since then, the Hamiltonians at different times do no longer commute, i. e. energy is no longer conserved, and \hat{B} would have to be expanded about t to get a more accurate approximation. Following [3], we now consider the quantity

$$S(\hat{A}, \hat{B}, \lambda) = e^{\lambda(\hat{A} + \hat{B})} \quad (3.3)$$

The idea of the split-step operator method is to expand the quantity S to some order that governs the global quality of the method. We can make an expansion about λ :

$$S(\hat{A}, \hat{B}, \lambda) = S_1(\hat{A}, \hat{B}, \lambda) + \frac{1}{2} [\hat{A}, \hat{B}] \lambda^2 + \dots \quad (3.4)$$

Where $S_1(\hat{A}, \hat{B}, \lambda) = e^{\lambda \hat{A}} e^{\lambda \hat{B}}$ One can further show [3, 21] that:

$$S(\hat{A}, \hat{B}, \lambda) = S_2(\hat{A}, \hat{B}, \lambda) + \frac{1}{24} [\hat{A} + 2\hat{B}, [\hat{A} + \hat{B}]] \lambda^3 + \mathcal{O}(\lambda^4) \quad (3.5)$$

with $S_2(\hat{A}, \hat{B}, \lambda) = e^{\lambda\hat{A}/2}e^{\lambda\hat{B}}e^{\lambda\hat{A}/2}$, which yields an approximation to second order using a symmetric decomposition. Going to higher orders usually involves finding imaginary roots of polynomials, which would introduce real quantities in the exponentials and consequently, those schemes do not conserve unitarity [3]. This paper also shows, that the quantity S_2 is actually accurate to third order for time-independent Hamiltonians, which stems from the fact that in this case the operators \hat{A} and \hat{B} do commute at different times. I found it not to be practical to go beyond the third-order approximation, since the main effect of the higher accuracy is to slow down the calculations, and one can well account for higher accuracy by simply cutting down the time step. This practice was also adopted by recent work in the field [7].

3.2 The Gross-Pitaevskii Equation

3.2.1 The Framework

We want to solve a nonlinear partial differential equation of the form:

$$i\frac{\partial\psi}{\partial t} = (\hat{A} + \hat{B})\psi \quad (3.6)$$

Where \hat{A} contains all the spatial derivatives and \hat{B} contains the potential terms that are in general functions of x and t . However, for time-independent potentials the exact solution of (3.6) would be:

$$\psi(x, t + \Delta t) = e^{\lambda(\hat{A} + \hat{B})}\psi(x, t) \quad (3.7)$$

Where $\lambda = i\Delta t$. Considering the above formulae, we are therefore confronted with the problem of splitting this time-independent exponential. [4] states that for such a problem, a symmetric product formula as the above to accuracy λ^{2n+1} can be given by the recursion scheme

$$e^{\lambda(\hat{A} + \hat{B})} = S_{2n+1} + \mathcal{O}(\lambda^{2n+1}) \quad (3.8)$$

$$\begin{aligned} S_{2n+1}(\lambda) &= S_{2n-1}(\lambda s_{2n+1})S_{2n-1}[\lambda(1 - 2s_{n+1})]S_{2n-1}(\lambda s_{2n+1}), \\ 2(s_{2n+1})^{2n-1} + (1 - 2s_{2n+1})^{2n-1} &= 0, \\ S_3(\lambda) &= e^{\lambda\frac{\hat{A}}{2}}e^{\lambda\hat{B}}e^{\lambda\frac{\hat{A}}{2}} \end{aligned} \quad (3.9)$$

now adapting the index to the overall accuracy for clarity. It has to be mentioned that these approximants have the advantage of being unitary, $S(\lambda)S(-\lambda) = 1$ and therefore conserve the norm of the function $\psi(x, t)$ at every time step. The roots of the polynomial (3.9) are such that certain commutators of \hat{A} and \hat{B} vanish. These roots can be imaginary when considering schemes of arbitrary precision and thus can introduce some real exponential which does no longer conserve the norm and

is therefore not very practicable for an imaginary differential equation. It is also important to note that S_3 already implies the calculation of three exponentials, S_5 has seven of them and S_7 has 19. Thus, the computational time needed diverges. [4] further shows that the accuracy for a given time step λ can be estimated to $\approx 10^{-6}$, for S_3 . Our scheme used is therefore given by:

$$e^{\lambda(\hat{A}+\hat{B})} \approx S_3 + \mathcal{O}(\lambda^3) \quad (3.10)$$

Still, this leaves us with the problem of calculating the exponential of an operator containing derivatives. Happily however, the Fourier-transform diagonalizes the operator $e^{\frac{\partial^2}{\partial x^2}}$, and we can carry out the calculation in Fourier space rather than having to carry out a matrix multiplication, so the scheme is of order $N \log N$ in the number of used points. We are now showing how to take a nonlinear Schrödinger equation apart. We start with:

$$i \frac{\partial \psi}{\partial t} = -\frac{\partial^2 \psi}{\partial x^2} + g|\psi|^2\psi + V(x)\psi \quad (3.11)$$

$$\psi(x, 0) = f(x) \quad (3.12)$$

By the special nature of the kick, we can regard the second term of the right-hand side of (3.11) as a time-independent potential, as only phase-factors are multiplied in, so a more accurate approximation is not needed. For a discretized system, the solution to the above equation to third order in Δt is given by:

$$\psi(x, t + \Delta t) = e^{-i \int_t^{t+\Delta t} \left(-\frac{\partial^2}{\partial x^2} + g|\psi|^2 + V(x) \right) dt} \psi(x, t) + \mathcal{O}(\Delta t^3) \quad (3.13)$$

Then, the exponential can be approximated to second order as:

$$e^{-i \int_t^{t+\Delta t} \left(-\frac{\partial^2}{\partial x^2} + g|\psi|^2 + V(x) \right) dt} = e^{-i \Delta t \left(-\frac{\partial^2}{\partial x^2} + g|\psi|^2 + V(x) \right)} \quad (3.14)$$

This is now our workable solution to propagating the Gross-Pitaevskii equation and forms the very fundament of every calculation done.

3.2.2 Finding the Groundstate Using the Split-Step Operator Method

To calculate the Groundstate of a Bose-Einstein condensate in an optical lattice, one has several possibilities. The method used was first to cast the Hamiltonian into its matrix representation, in order to diagonalize it using the LAPACK subroutine DSTEV. However, this proved not favourable when considering large couplings, where the system would only slowly converge, if convergence occurred at all, and each step involved diagonalizing a whole matrix of linear dimension ~ 1024 , while only the lowest eigenvector was needed. Mainly for this shortcoming, another technique was implemented. When using the split-operator

technique as described above and propagating in imaginary time, $\tau = it$, the system is obviously no longer normalized. However when renormalizing after each imaginary time step, one gradually approaches the exact groundstate. Up to coupling strengths of 10, 20000 iterations proved sufficient to get a groundstate that would by later propagation not alter its nature, nor its momentum profile. In this manner, one always applies the same operator to the wavefunction, even when propagating in real time, which of course adds to numerical stability. Recent work uses more sophisticated methods such as DDS [13], and Collocation with Legendre-Polynomials [5], mainly for the fact that the scheme presented here does not scale very well and is actually quite slow when going to higher dimensions.

Propagation in Imaginary Time

The method of choice applies predominantly to linear systems, yet it can be shown that one can use the same technique for nonlinear Schrödinger equations (NLSEs). We start with the linear case. Our procedure is to apply the operator $\mathcal{T}(\tau) = e^{-\tau \hat{H}}$ to some given initial state $|\psi_0\rangle$. The obtained state is subsequently normalized and we obtain an iterative procedure:

$$|\psi_{n+1}\rangle = \frac{\mathcal{T}(\tau)|\psi_n\rangle}{\sqrt{\langle\psi_n|\mathcal{T}(\tau)|\mathcal{T}(\tau)\psi_n\rangle}} \quad (3.15)$$

Let us now assume that the eigenstates to the Hamiltonian are known, so that we may express $|\psi_n\rangle$ in terms of these eigenstates, $|\psi_n\rangle = \sum_i c_i |\phi_i\rangle$, and that the corresponding eigenvalues are ordered such that $|\lambda_0| < |\lambda_1| < \dots$. Then, the right-hand side of (3.15) can be cast in the form:

$$\begin{aligned} \frac{\mathcal{T}(\tau)|\psi_n\rangle}{\sqrt{\langle\psi_n|\mathcal{T}(\tau)|\mathcal{T}(\tau)\psi_n\rangle}} &= \frac{\sum_i c_i \mathcal{T}(\tau)|\phi_i\rangle}{\sqrt{\sum_{i,j} c_i^* c_j \langle\phi_i|\mathcal{T}(\tau)\mathcal{T}(\tau)|\phi_j\rangle}} \\ &= \frac{\sum_i c_i e^{-\tau\lambda_i} |\phi_i\rangle}{\sqrt{\sum_i |c_i|^2 e^{-2\tau\lambda_i}}} \\ &= \frac{\sum_i c_i e^{-\tau\lambda_i} |\phi_i\rangle}{\sqrt{\sum_i |c_i|^2 e^{-2\tau\lambda_i}}} \cdot \frac{e^{\tau\lambda_0}}{e^{\tau\lambda_0}} \\ &= \frac{\sum_i c_i e^{-\tau(\lambda_i - \lambda_0)} |\phi_i\rangle}{\sqrt{\sum_i |c_i|^2 e^{-2\tau(\lambda_i - \lambda_0)}}} \end{aligned}$$

Thus, since by our assumption the exponents remain negative for all $i \neq 0$, one can readily see that this procedure amplifies the groundstate $|\phi_0\rangle$, so that, as $\tau \rightarrow \infty$, the system will be in its groundstate. This proof does however only apply to the linear case. Its nonlinear generalization requires an additional component to the ground state, $|\tilde{\phi}\rangle$, obviously satisfying $\langle\tilde{\phi}|\hat{H}|\tilde{\phi}\rangle \leq \lambda_1$, since

then, our method is still valid, with the assumption that there is a gap between this state and the first excited state, and therefore a discrete spectrum even for the nonlinear case. It can readily be shown, that the energy levels of the Gross-Pitaevskii equation are indeed discrete¹, so our method is well applicable here. Using this method, one effectively finds the groundstate for arbitrary coupling constants.

3.3 The Code

3.3.1 C++-Code for the Split-Step Operator Method

One of the main goals of this work was to obtain working code that is sufficiently fast to yield results with a decent accuracy. All the papers cited so far exhibit their results, yet few do comment on the method or code used, which slows down the overall implementation since one has to reinvent the wheel. Most of the code accompanying this work was used for testing, particularly the code in the `oldcode` directory, which was used to develop a feeling for the split-step operator method. The main Files needed are `split_step.h`, `BEC_Groundstate.h` and `fft.h`. The first two implement templated functions and classes to do the timesteps and to find the Groundstate. Provision is made for the Groundstate solver to use the Lanczos-Algorithm of the IETL, which can be introduced by simply implementing the functions needed. The file `fft.h` contains a C++ wrapper function for the well known FFTW-library to execute fourier Transforms. The code will not compile on a system, where fftw Version 3.0.1 is not installed. Also, the code makes use of some data-structures from the Boost-library, namely uBlas-matrices for the LAPACK routines. At present however, the programs can do without, when finding the groundstate with the relaxation method. The working of the programs is in short summarized by the following steps:

1. Parse command line arguments (kick strength, coupling strength, maximum time, Δt , number of points) if given.
2. Find the groundstate and normalize.
3. Kick as needed.
4. **for** $t < \text{maxt}$, $++t$ **do**:


```

        split_step
        if not(t%period)
          print data
        fi
      done
```

¹For a proof for sufficiently smooth potentials, the reader is referred to [12]

The output is directed to standard output, whence it can be redirected to any file by using the shell of choice.

3.3.2 Perl code

In order to optimize the calculation time used on the Asgard Beowulf cluster of the ETH, I wrote code that printed various data. In order to analyze these files, I wrote a small perl script, `analyze`, which allowed to do some statistics with calculated histograms. The script `scripter.pl` was used to create PBS jobs on Asgard, taking as command-line arguments the processors needed, the number of nodes and the walltime. The analysis of the histogram data is treated further on in the text.

Chapter 4

Results

4.1 The System under consideration

As was pointed out above, the goal was to implement the simulation of a Bose-Einstein condensate that obeys Gross-Pitaevskii dynamics and is trapped in some harmonic trap with a lattice superimposed to it. The ground state is found using imaginary time propagation. As soon as the ground state is reached, a kick of the form $K \sin(x)$ is exerted on the system, which is in turn propagated for a certain time afterwards. As was shown, the main effect of the kick is to shift the peak of the momentum distribution to the right. However, when kicks become strong enough, the system shows a rapid decoherence, in that the momentum distribution begins to spread out very rapidly over the whole spectrum. Our system follows the equation

$$i \frac{\partial \psi}{\partial t} = \left(-\frac{1}{2} \frac{\partial^2}{\partial x^2} + g|\psi|^2 + \frac{1}{2}x^2 + \frac{q_B^2}{2} \sin^2(qx) \right) \psi \quad (4.1)$$

where q_B and q are as was already mentioned the momentum at the Brillouin-zone boundary and the reciprocal lattice constant, respectively.

4.2 “Phase Space” Plots of the BEC

In order to visualize the transition to chaotic behaviour in the first place, and to find out what kick strengths are needed for the system to become unstable, one can use a technique familiar from classical mechanics on the following grounds: Without interaction between the atoms, the BEC can be seen as a normal harmonic oscillator, treated quantum mechanically. As the only new physics are a discrete energy spectrum and a probability amplitude instead of a trajectory, the system remains stable in the sense that the peak of position and momentum distributions oscillate back and forth, and are reflected at the walls of the trap. Thus, one can visualize the system in a “phase space” for mean position and

mean momentum. If the system is stable, the oscillation of mean position ($\langle x \rangle$) and mean momentum ($\langle p \rangle$) can be seen as the trajectory of a normal oscillator, describing a circle. When becoming unstable however, the time dependence of the above averages should no longer follow simple curves and consequently fill up all of the phase space. Figure 4.1 shows the same system kicked with various strengths to illustrate the stability of the system for small K .

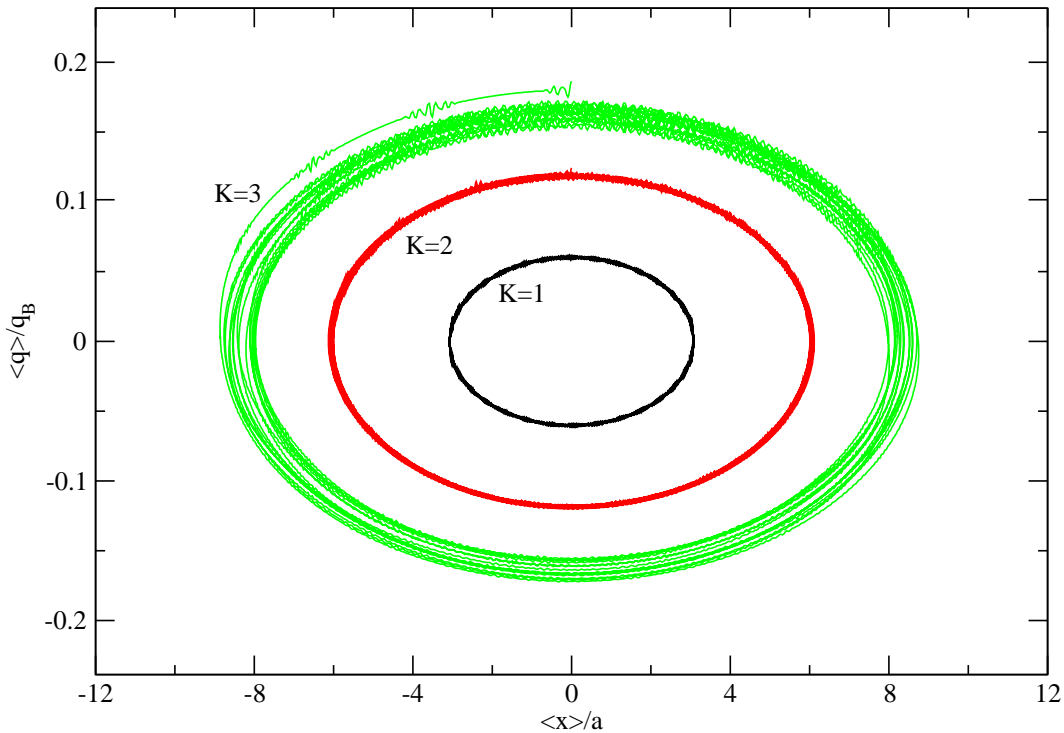


Figure 4.1: Mean position versus mean momentum for various values of K . The interaction is set to $g = 0.1$.

If one subsequently applies a larger kick, e.g. $K = 6$, the system becomes unstable. The mean momentum and mean position do no longer oscillate, as Figure 4.2 indicates. The coupling strength g was deliberately kept at a low value so as not to introduce too much numerical “noise”. It is seen that transition to chaos eventually occurs, since it is the nonlinearity that eventually drives the system to instability, when kicked hard enough. Naturally, as will be shown

below, for larger values of g , the system will “surrend” at smaller K .

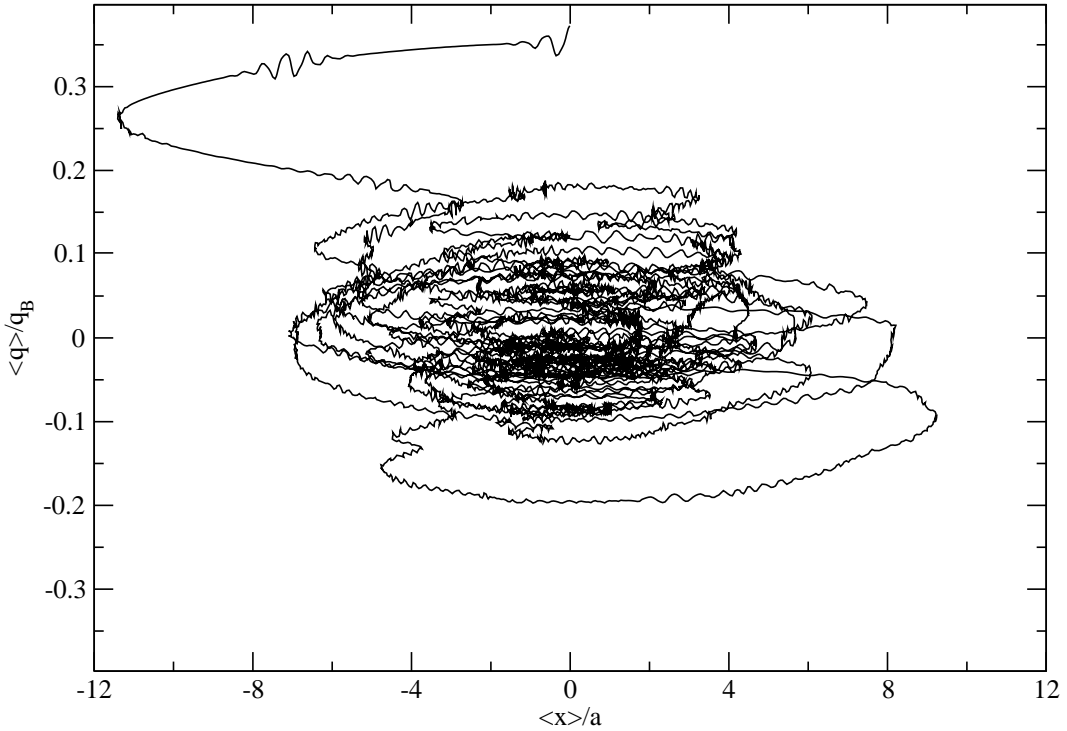


Figure 4.2: Mean position versus mean momentum for $K = 6$. The interaction is set to $g = 0.1$.

The following figure shows the same behaviour but without the lattice underneath. Note that the results are very similar, since, as was seen before, in coordinate space the effect of the lattice is to produce wiggles in the distribution and satellite peaks in momentum space, so when averaging over all values, one basically recovers the same results. These pictures do only show that the system can be made unstable by kicking strong enough, yet nothing is known about the way the momenta are distributed:

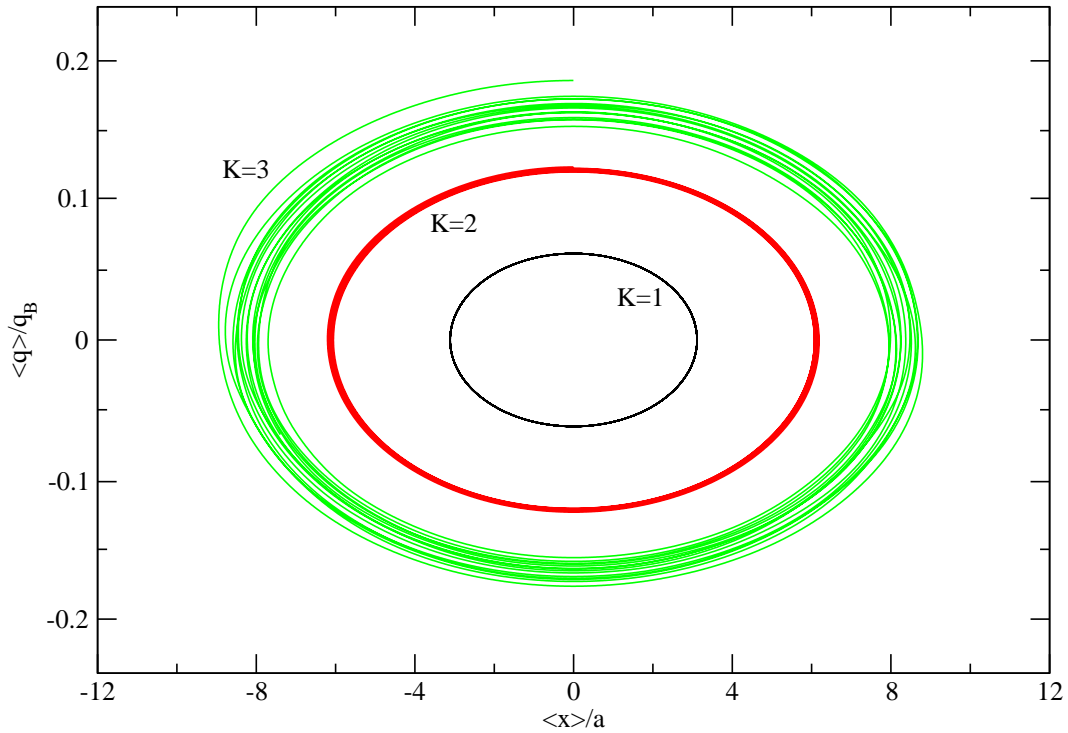


Figure 4.3: Mean position versus mean momentum for various values of K . The interaction is set to $g = 0.1$. The main effect of the lattice is to introduce wiggles.

4.3 Momentum Distributions at Various Times

It was put forward that at a given kick strength, the system at hand shows phase decoherence, which expresses itself in a momentum distribution that ‘smears’ out. Apart from truncation errors, momenta spread out over the whole Brillouin zone of the lattice. Figure 4.4 shows this behaviour. As time passes, the distribution gets wider. The widening of the spectrum is not clearly seen from this figure, yet it was added to show time propagation of the distribution and to visualize the behaviour of the BEC when kicked. Already at the moment of the kick ($t = 0$), one can see decoherence in momentum space, as the kick is strong enough. As time passes, the momenta spread out over essentially the whole Brillouin-zone and we have a decoherent system. [8] produced such a system in 2002 by applying a

magnetic field gradient to a BEC and afterwards found the system in a dephased state. A better technique for analyzing the widening of the distributions will be presented later in the text.

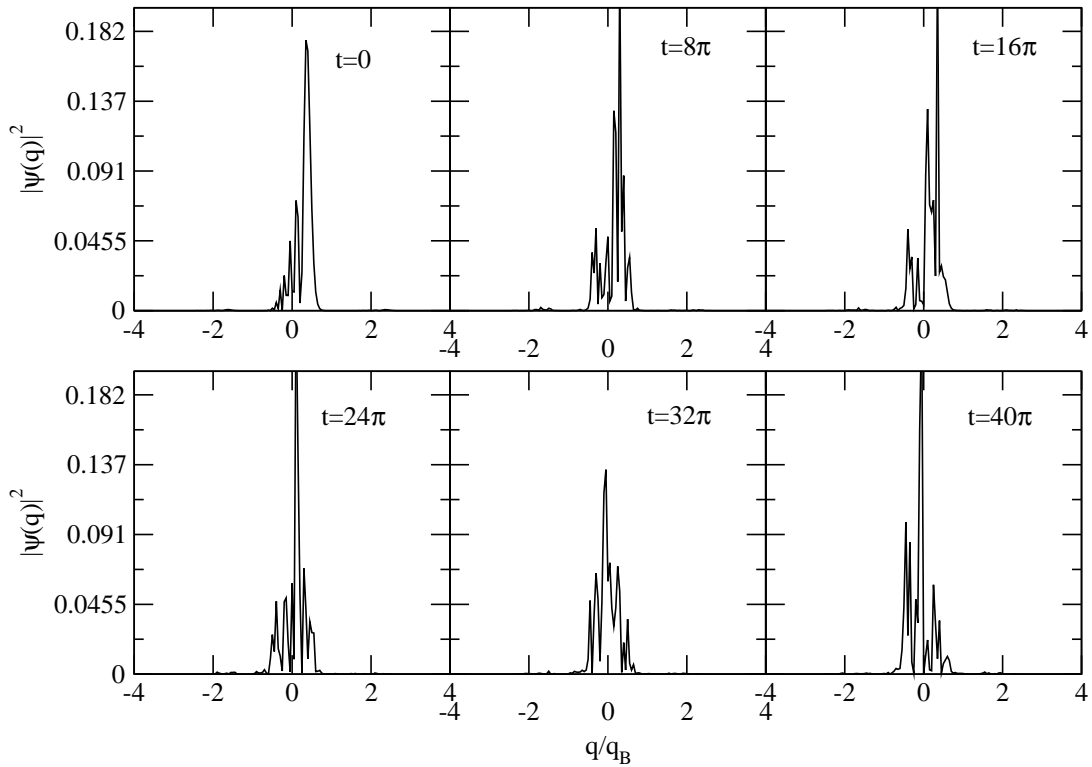


Figure 4.4: Momentum distribution after kicking with $K = 6$ and $g = 5$, at different times. The orders of magnitude are clearly decreasing.

In order to quantify in some way the broadening of the spectrum with increasing K , one has to resort to an averaging over time that does not focus on some given moment in time, but rather takes into account the developement of the past as well. Having such an average, one can quite definitely make predictions about in what way the momenta spread. In the following section, an averaging technique borrowed from electrical engineering and econometrics is introduced and used to look at momentum distributions at various times.

4.4 Widths of Momentum Distributions

4.4.1 The Exponentially Weighted Moving Average.

In averaging the distributions, I used a so-called exponentially weighted moving average (EWMA), which is used when placing more weight on more recent data. Let x_k be some measurement at time k . The normal moving average is formed by:

$$\bar{x}_k = \frac{1}{n} \sum_{i=k-n+1}^k x_i \quad (4.2)$$

Taking one additional point, this becomes:

$$\begin{aligned} \bar{x}_{k+1} &= \frac{1}{n+1} \sum_{i=k-n+1}^{k+1} x_i \\ &= \frac{1}{n+1} [x_{k+1} + n\bar{x}_k] \\ &= \frac{1}{n+1} x_{k+1} + \frac{n}{n+1} \bar{x}_k \end{aligned} \quad (4.3)$$

Let now the filter-constant be $\alpha = \frac{n}{n+1}$. Naturally, for $n > 1$, $\alpha < 1$. The exponentially weighted moving average is then formed by calculating:

$$\bar{x}_{k+1} = \alpha \bar{x}_k + (1 - \alpha) x_{k+1} \quad (4.4)$$

where x_{k+1} is the value of x at time $k + 1$. The value \bar{x}_{k+1} is then taken to be the real value, which has now filtered out truncation errors that come from finite machine precision. Upon further expansion backwards, it is easily seen, that the most recent value or distribution in our case gets the biggest weight, whereas the other distributions are weighted with higher powers of α . Hence the name “exponentially weighted”. It is a means for weighting the more recent data more heavily than the past ones, while still “remembering” them. For further details the reader is referred to [22]. With this momentum distributions, it is seen that as the kick gets stronger, the width of the distribution increases. This is the same phenomenon which is seen in figure 4.4, and the main result of my analysis.

4.4.2 Widths

Using the EWMA, the distribution at each time step was averaged in the sense above, replacing the filtered value with the actual one at a given time. Then, at given intervals of 2π , the distributions were printed out yielding a series of distributions for a given kick strength. For each of those distributions, the variance was measured, and subsequently averaged. Furthermore, the mean deviation of the variance so obtained was calculated, which is shown as an error bar for each data

point in the following figures. Figure 4.6 shows the mean variance ($\langle \sigma \rangle$) of the momentum distribution averaged over time for a given kick strength. Figure 4.5 should give some impression on how the distributions were averaged.

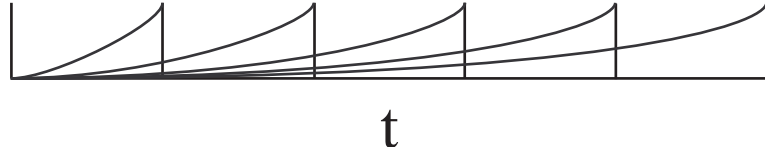


Figure 4.5: EWMA. The actual distribution was replaced by an EWMA distribution that takes into account the history of the condensate. The weight is increasing towards the distribution that is considered.

As the error bars indicate, this quantity does not fluctuate much, yet the with rising K , one observes a broadening of the momentum distribution. As was mentioned before, the main effect of the nonlinearity is to broaden the “cloud” of the condensate as a whole. Consequently, the momentum distribution is narrower than for a noninteracting system. In the figures following, one can clearly see that the curve for $g = 5$ lies lower than the one for $g = 1$.

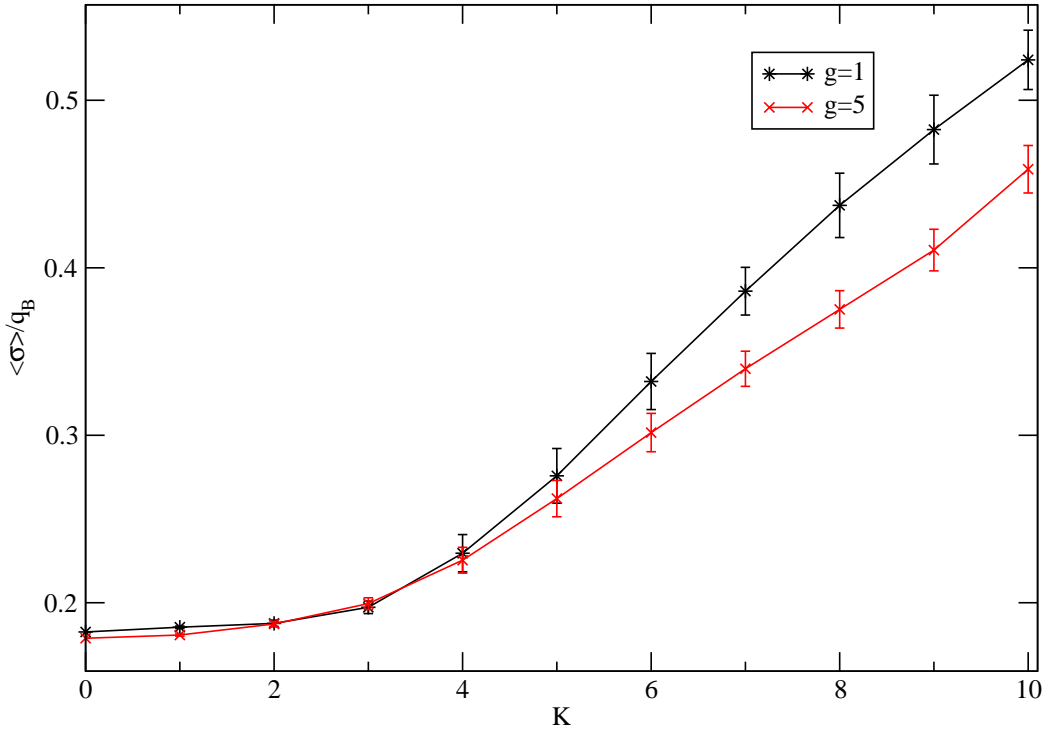


Figure 4.6: Time-averaged width of the momentum histograms as a function of K .

As figure 4.6 suggests, for small K , The width does not alter nor does it vary much. This is consistent with the observation that the mean momentum basically oscillates between two extreme values of the same order of magnitude as was calculated by using the variational approach. Figure 4.7 shows this fact. However, this oscillatory pattern is distorted when going to $K = 3$, and the instability sets in at $K \sim 4$, as the subsequent figures show.

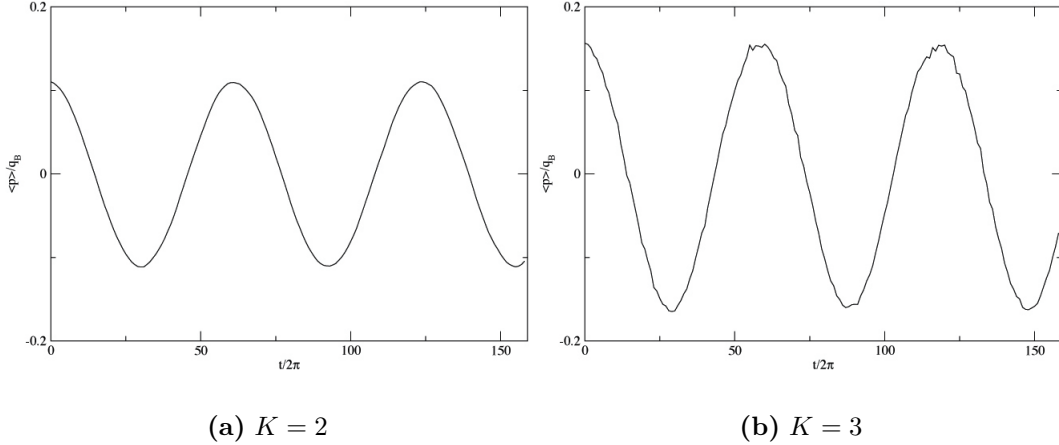


Figure 4.7: Mean momentum of a BEC in a lattice when kicked with different kick strengths, $g = 1$

It is clear that when exerting a kick to the condensate, one obviously enhances momenta and consequently, the energy of the system is augmented by a factor that is proportional to the kick strength squared. However this energy competes with the interaction energy. If the Interaction term is strong enough, transition to a Mott-insulator state can occur [8, 11], which is however no longer governed by the Gross-Pitaevskii equation, yet it is of course another instance of a state showing phase decoherence, as the atoms arrange in a way as to fill the lattice, having commensurate filling on the lattice sites. Our system can be considered in second quantized notation:

$$\hat{H} = -J \sum_{\langle i,j \rangle} \hat{a}_i^\dagger \hat{a}_j + \sum_i \varepsilon_i \hat{n}_i + \frac{1}{2} U \sum_i \hat{n}_i (\hat{n}_i - 1) \quad (4.5)$$

which is a Bose-Hubbard model [11]. J is the tunneling (or hopping) matrix element between two adjacent sites and ε_i is the energy offset due to the external potential. U is the familiar on-site interaction between the atoms. For this system, it can be shown that a transition to a Mott-insulator occurs if $\frac{U}{J} = z \cdot 5.8$, where z is the number of nearest neighbours. The system in our application is at all times far off this critical limit, as the lattice potential is greater than U by one order of magnitude, yet the decoherency is visible and is a result of the nonlinearity of the Gross-Pitaevskii equation, as was already mentioned. It is also shown in [8] that a decoherency produced in this way does not vanish, even when the trap potential is switched off adiabatically, in contrast to the Mott-insulator state, where coherence is rapidly restored. This indicates that the decoherence is due to the physics of the system (i.e. the Gross-Pitaevskii equation) and not due to a dephasing of the condensate wavefunction, which would eventually restore the interference pattern.

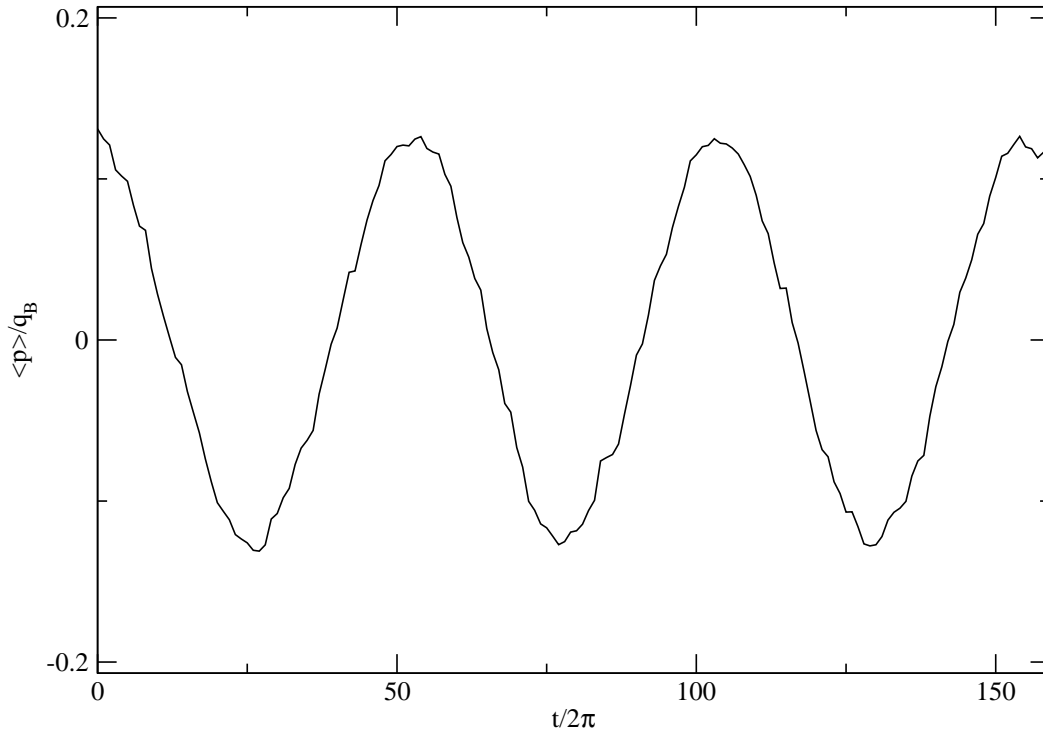


Figure 4.8: Mean momentum of a BEC in a lattice when kicked with $K = 3$, $g = 5$.

When doubling the points used in the calculations or cutting the timestep Δt by half, one recovers essentially the same pattern, as figure 4.9 shows. However, the noise in the pattern stems from the kick, which shows that instability slowly sets in.

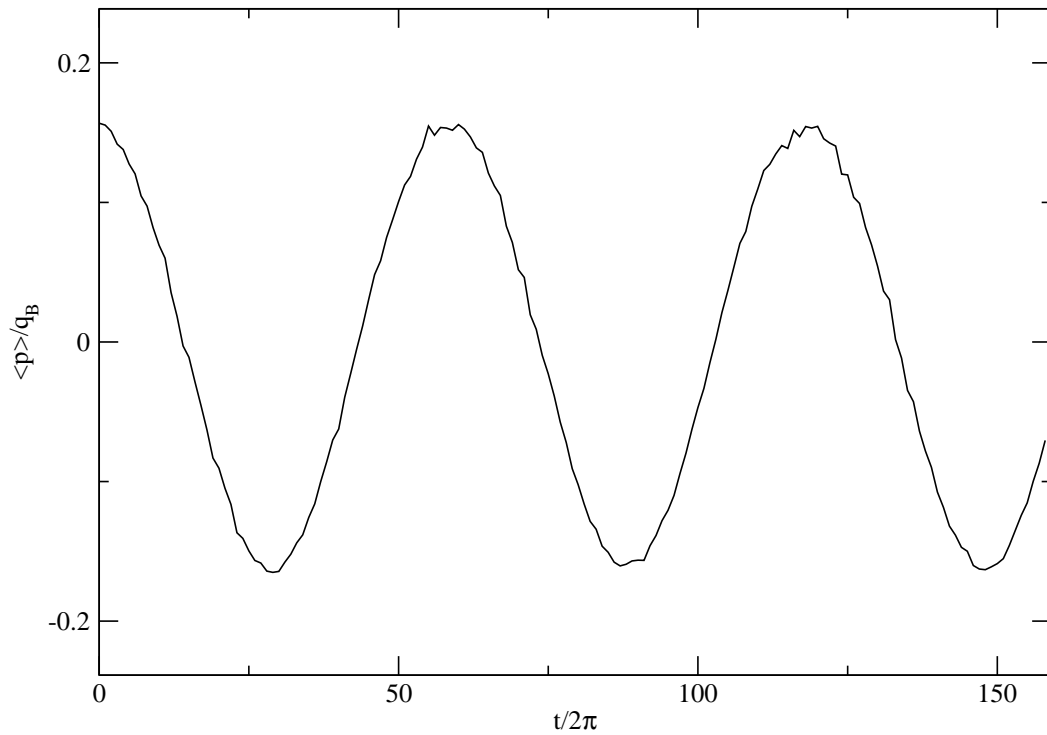


Figure 4.9: Mean momentum of a BEC in a lattice when kicked with $K = 3$, $g = 5$, but with half the timestep and doubled number of points.

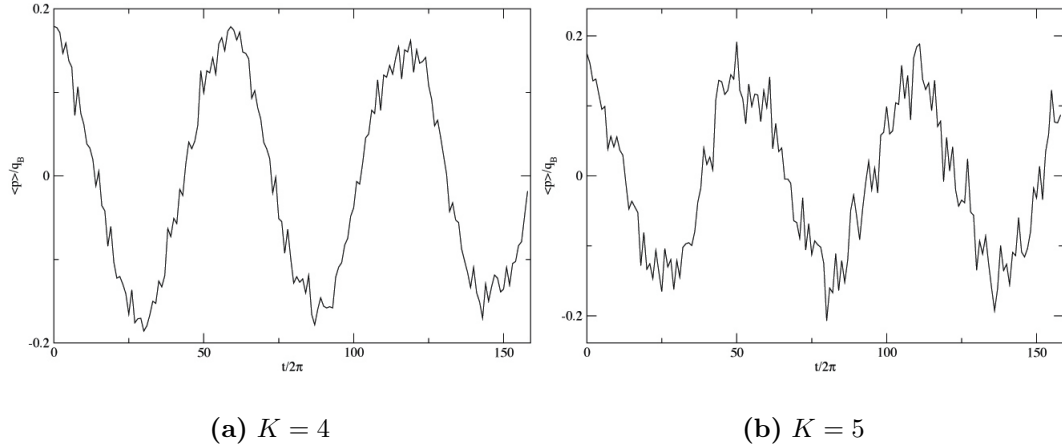


Figure 4.10: Mean momentum of a BEC in a lattice when kicked with different kick strengths, $g = 1$

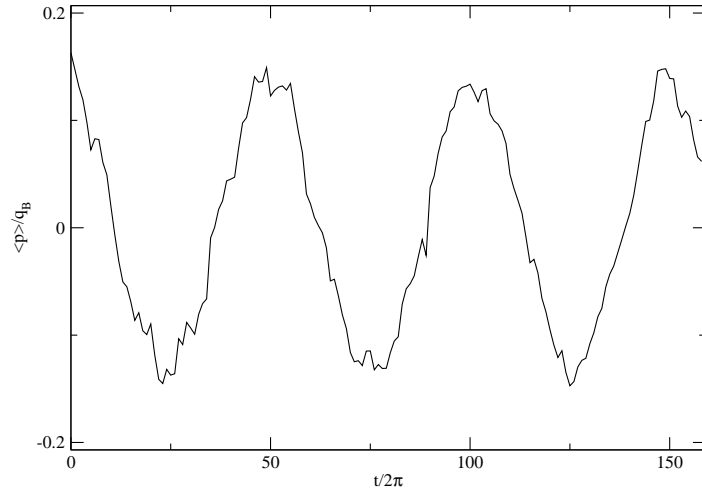


Figure 4.11: Mean momentum of a BEC in a lattice when kicked with $K = 4$, $g = 5$.

The oscillatory pattern in the above figures is due to the lattice, but when the system is kicked strong enough, one can effectively drive the system to a completely unstable state, as is shown in the next plot.

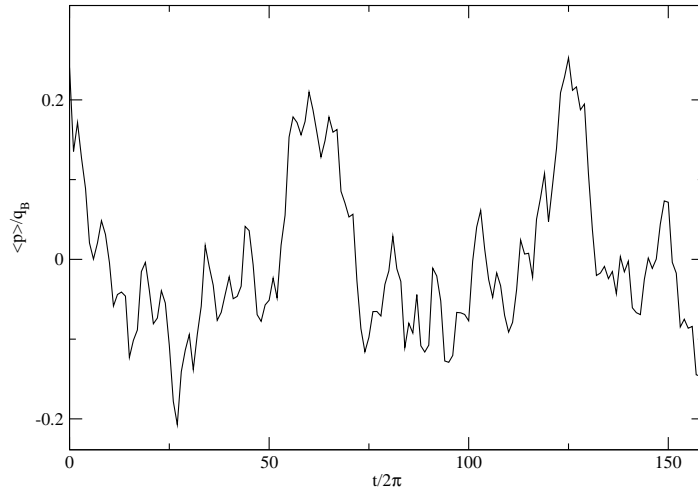


Figure 4.12: Mean momentum of a BEC in a lattice when kicked with $K = 8, g = 1$.

These figures suggest a critical value of K between 3 and 4. If one leaves away the lattice the initial width is considerably smaller, the distribution not having satellite peaks. Even without a lattice, one can prepare an instable system. The effect of the lattice is, as was pointed out above and as can be seen in figures 1.1 and 1.2, to introduce wiggles in the wavefunction. The lattice sites tend to bind the atoms of the condensate. If one leaves away the lattice, there should not be any changes to the behaviour for large kick strengths, since, as was pointed out by Greiner et. al. [8], a decoherent system that is not produced by transferring it to a Mott-insulator, stays decoherent when obeying the Gross-Pitaevskii equation.

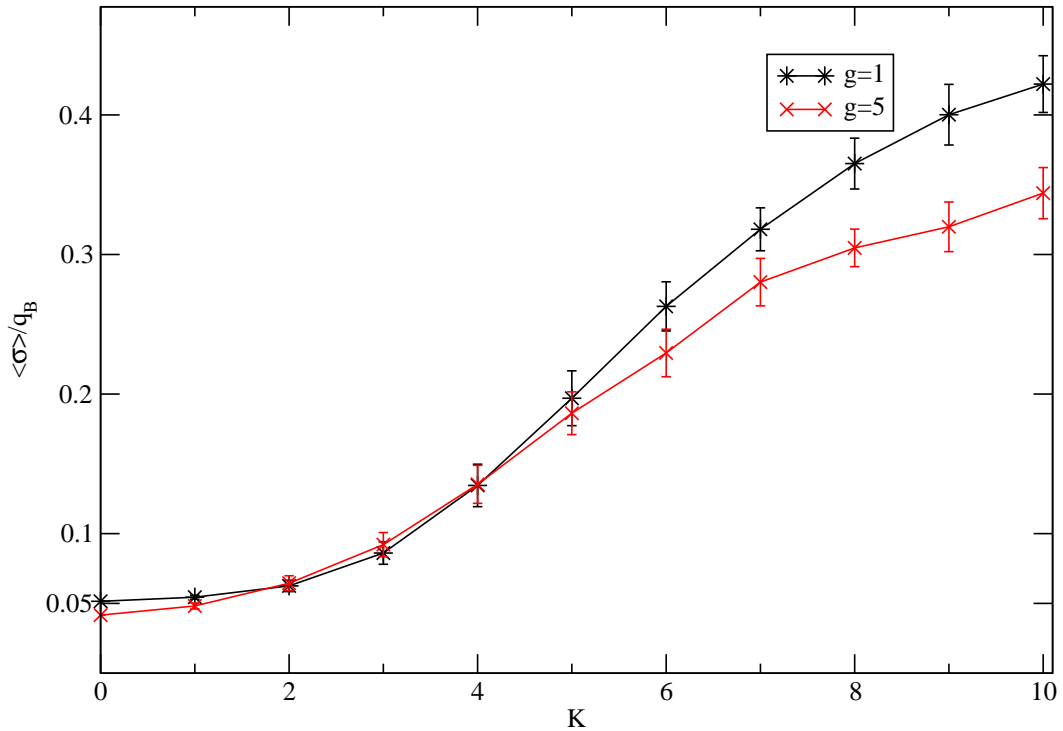


Figure 4.13: Time-averaged width of the momentum histograms as a function of K , without lattice.

The corresponding plots for a condensate in a trap without a lattice and for a free condensate have also been included. It seems to be striking that the lattice is introducing or rather accentuating levels at which the width does not change when being exposed to a larger kick. This fact could be the subject of further investigation. When kicking either a free condensate or one in an optical lattice for that matter, one has to bear in mind that the simulation cannot realize an infinite system, but still there are periodic boundaries, whose effects now become more important. One of those effects is to still confine the wavefunction, since the condensate wavefunction would not be an element of the Hilbert space and therefore non-physical. Thus, when applying rigid walls no matter how far away, the wavefunction will be of a cosine form and therefore, the kick will still have the same effect of shifting the momentum distribution to the right and consequently, the spectrum is widened. When there is a lattice in addition, there will be a

stabilizing effect for the reasons already cited.

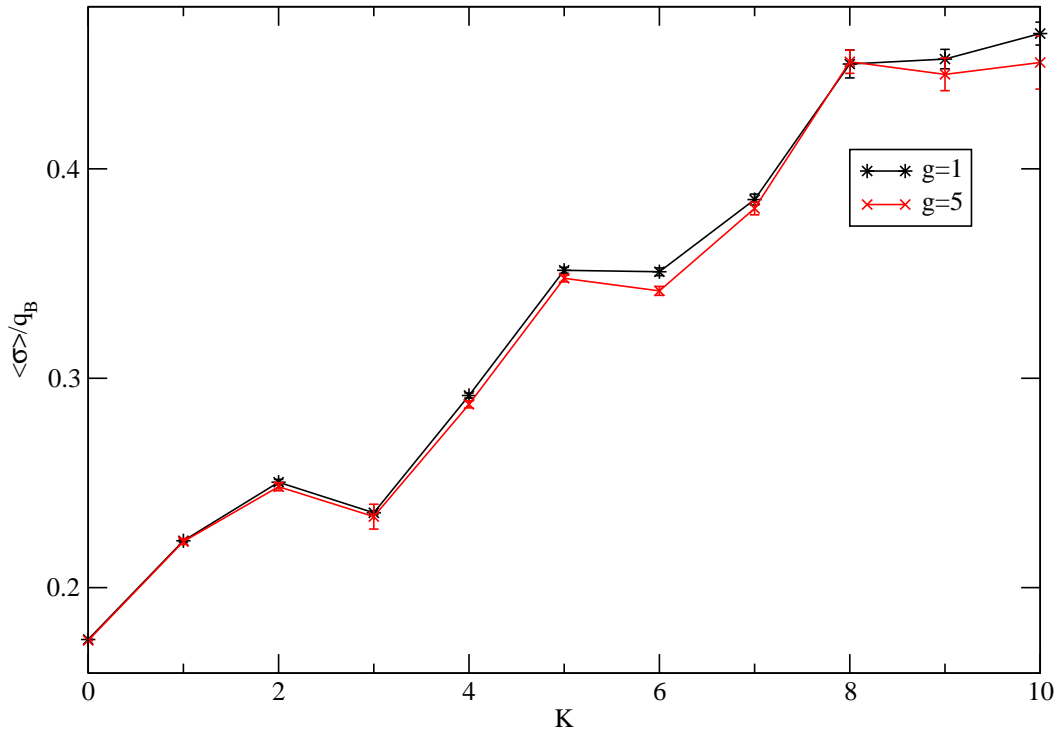


Figure 4.14: Time-averaged width of the momentum histograms as a function of K , without a trap.

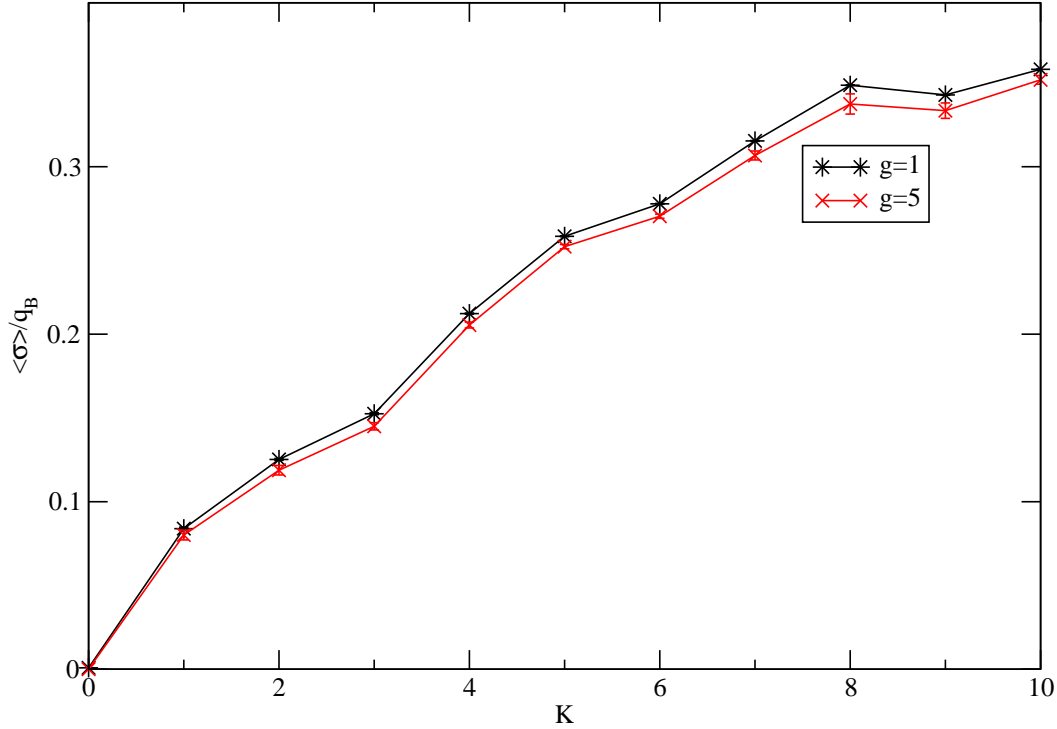


Figure 4.15: Time-averaged width of the momentum histograms as a function of K for a free condensate.

Parameters

Usually, $N = 1024$ points proved to be enough points to give sensible results. Going to larger systems mainly increases runtime of the programs. The timestep was measured in units of 2π , where it proved sufficient to divide this interval by 10^4 .

4.5 Conclusion

Using the split-step operator technique to solve nonlinear partial differential equations, a one-dimensional Bose-Einstein condensate in a trap with a lattice was simulated. Kicks of various strengths have been applied and the system was

shown to undergo a transition to instability after applying the kick. This can be seen best by considering the momentum distribution and its width when averaged over time. While in the stationary case, momenta are locked, the kick leads to a decoherence in momentum space. This accounts for the fact that the width of the momentum spectrum increases, when larger kicks are exerted. The system is very similar to that found by Greiner et. al. [8], in that when exerting a kick, one dephases the system by an onset of additional energy proportional to K^2 . This energy, which is initially purely kinetic, tends to compete with the interaction energy. Kinetic energy raises the tunneling amplitude for the lattice. In consequence however, the interaction energy is raised. [8] has shown that for lattices that are deep enough, a system rapidly undergoes a phase transition to a Mott-insulator state for the fact that the tunneling amplitude is comparable to the interaction energy. This is a decoherent state, since there are exactly the same number of atoms on each lattice site, which accounts for an essentially flat momentum histogram by the Heisenberg uncertainty principle. However, coherence is restored a few milliseconds after switching off (or reducing) the potential, whereas for a system that was prepared to be decoherent by ways of e.g. a kick, this does not happen, since the decoherence stays “intact” by the nonlinearity of the Gross-Pitaevskii equation governing the Bose-Einstein condensate. Some plots of a somewhat artificial phase space have been added to show this unstable behaviour in terms of mean momentum and mean position. At the onset of the instability, the system of course tends to cover the whole phase space, which again accounts for the fact that when a system becomes unstable, mean momentum and mean position can take all possible values allowed by the overall energy of the system. This again expresses the fact of decoherence, as when momena are randomly distributed over the Brillouin-zone, so is its mean value.

Acknowledgements

I would like to thank Prof. Dr. Matthias Troyer for assigning me to a very interesting and challenging work in Computational Physics, which surely is to become one of the most active fields of research in years to come. My special thanks go to Dr. Stefan Wessel for all his encouraging discussions and especially for having patience with me.

List of Figures

1.1	Ground state distribution of a Bose-Einstein condensate in a periodic potential and its corresponding momentum distribution with $g = 1$	8
1.2	Same as figure 1.1 with $g = 5$	9
1.3	Average energy of a BEC confined to a ring. The nonlinearity destroys quantum anti-resonance. Taken from [23]	10
1.4	A one dimensional Bose-Einstein Condensate kicked with a strength $K = 1$. Note the slight shift to the right. With the <code>analyze</code> Perl script, the mean momentum was found to be $\langle p \rangle = 0.778801$, which in the above units is at roughly 0.06 and $\langle p^2 \rangle - \langle p \rangle^2 = 0.577409$, which would be about 0.05. Although no Brillouin-zone is present, I chose to normalize with the Brillouin vector, in order to get rid of factors of π	12
1.5	A one-dimensional BEC kicked with $K = 5$, $\langle p \rangle \approx 0.19$ and $\langle p^2 \rangle - \langle p \rangle^2 \approx 0.09$	13
2.1	The effect of a finite inter-particle interaction is to move the atoms apart. For the particular normalization to unity, the dependence is approximately linear.	21
2.2	Ground state distributions for two different interaction strengths. No optical lattice has yet been applied	22
4.1	Mean position versus mean momentum for various values of K. The interaction is set to $g = 0.1$	30
4.2	Mean position versus mean momentum for $K = 6$. The interaction is set to $g = 0.1$	31
4.3	Mean position versus mean momentum for various values of K. The interaction is set to $g = 0.1$. The main effect of the lattice is to introduce wiggles.	32
4.4	Momentum distribution after kicking with $K = 6$ and $g = 5$, at different times. The orders of magnitude are clearly decreasing. .	33

4.5	EWMA. The actual distribution was replaced by an EWMA distribution that takes into account the history of the condensate. The weight is increasing towards the distribution that is considered.	35
4.6	Time-averaged width of the momentum histograms as a function of K .	36
4.7	Mean momentum of a BEC in a lattice when kicked with different kick strengths, $g = 1$	37
4.8	Mean momentum of a BEC in a lattice when kicked with $K = 3$, $g = 5$.	38
4.9	Mean momentum of a BEC in a lattice when kicked with $K = 3$, $g = 5$, but with half the timestep and doubled number of points.	39
4.10	Mean momentum of a BEC in a lattice when kicked with different kick strengths, $g = 1$	40
4.11	Mean momentum of a BEC in a lattice when kicked with $K = 4$, $g = 5$.	40
4.12	Mean momentum of a BEC in a lattice when kicked with $K = 8$, $g = 1$.	41
4.13	Time-averaged width of the momentum histograms as a function of K , without lattice.	42
4.14	Time-averaged width of the momentum histograms as a function of K , without a trap.	43
4.15	Time-averaged width of the momentum histograms as a function of K for a free condensate.	44

Bibliography

- [1] M. H. Anderson, J. R. Ensher, M. R. Matthews, C. E. Wieman, and E. A. Cornell. Observation of bose-einstein condensation in a dilute atomic vapor. *Science*, 269:198, 1995.
- [2] V. I. Arnol'd. *Mathematical Methods of Classical Mechanics*. Springer Verlag, New York, 1989.
- [3] André. D. Bandrauk and Hai Shen. Improved exponential split operator method for solving the time-dependent schrödinger equation. *Chem.Phys. Lett*, 176:428, 1991.
- [4] André. D. Bandrauk and Hai Shen. Exponential split operator methods for solving coupled time-dependent schrödinger equations. *J. Chem. Phys.*, 99:1185, 1993.
- [5] Y.-S. Choi, J. Javainen, I. Koltracht, M. Kostrun, P. J. McKenna, and N. Savytska. A fast algorithm for the solution of the time-independent gross-pitaevskii equation. *J. Comp. Phys.*, 190:1, 2003.
- [6] A. Derevianko, W. R. Johnson, M. S. Safronova, and J. F. Babb. High-precision calculations of dispersion coefficients, static dipole polarizabilities, and atom-wall interaction constants for alkali-metal atoms. *Phys. Rev. Lett.*, 82:3589, 1999.
- [7] S. A. Gardiner, D. Jaksch, R. Dum, J. I. Cirac, and P. Zoller. Nonlinear matter wave dynamics with a chaotic potential. *Phys. Rev. A*, 62:023612, 2000.
- [8] M. Greiner, O. Mandel, T. Esslinger, T. W. Hänsch, and I. Bloch. Quantum phase transition from a superfluid to a mott insulator in a gas of ultracold atoms. *Nature*, 415:39, 2002.
- [9] P. C. Hohenberg. Existence of long-range order in one and two dimensions. *Phys. Rev. Lett.*, 17:1133, 1966.
- [10] K. Huang. *Statistical Mechanics*. John Wyley, New York, 1987.

- [11] D. Jaksch, C. Bruder, J. I. Cirac, C. W. Gardiner, and P. Zoller. Cold bosonic atoms in optical lattices. *Phys. Rev. Lett.*, 81:3108, 1998.
- [12] V. V. Konotop and P. G. Kevrekidis. Bohr-Sommerfeld Quantization Condition for the Gross-Pitaevskii Equation. *Phys. Rev. Lett.*, 91:230402, December 2003.
- [13] M. Kostrun and J. Javainen. An alternative numerical method for initial value problems involving the contact nonlinear hamiltonians. *J. Comp. Phys.*, 172:298, 2001.
- [14] C. Menotti, A. Smerzi, and A. Trombettoni. Superfluid dynamics of a bose-einstein condensate in a periodic potential. *New. J. Phys.*, 5:112.1, 2003.
- [15] N. D. Mermin and H. Wagner. Absence of ferromagnetism or antiferromagnetism in one- or two-dimensional isotropic heisenberg models. *Physical Review*, 158:383, 1967.
- [16] H. Moritz, T. Stöfele, M. Köhl, and T. Esslinger. Exciting collective oscillations in a trapped 1d gas. *Phys. Rev. Lett.*, 91:250402, 2003.
- [17] C. J. Pethik and H. Smith. *Bose-Einstein Condensation in Dilute Gases*. Cambridge University Press, Cambridge, 2002.
- [18] L. Pitaevskii and S. Stringari. *Bose-Einstein Condensation*. Clarendon Press, Oxford, 2003.
- [19] L. E. Reichl. *The Transition to Chaos In Conservative Classical Systems: Quantum Manifestations*. Springer-Verlag, New York, 1992.
- [20] F. Schwabl. *Quantenmechanik*. Springer-Verlag, Berlin, 1998.
- [21] M. Suzuki. General theory of higher-order decomposition of exponential operators and symplectic integrators. *Phys. Lett. A*, 165:387, 1992.
- [22] M. T. Tham, 1998. <http://lorien/ncl.ac.uk/ming/filter/filewma.htm>.
- [23] C. Zhang, J. Liu, M. Raizen, and Q. Niu. Transition to instability in a kicked bose-einstein condensate. 2003.